AMERICAN UNIVERSITY OF BEIRUT

ASSESSING THE OPERATIONAL LIMITS OF THE INTENSIFICATION OF CARBON CAPTURE BY ALKALINE SOLUTIONS

by
IBRAHIM GEORGES SALAMOUN

A thesis
submitted in partial fulfillment of the requirements
for the degree of Master of Chemical Engineering
to the Baha and Walid Bassatne Department of Chemical Engineering
and Advanced Energy
of the Maroun Semaan Faculty of Engineering and Architecture
at the American University of Beirut

Beirut, Lebanon
February 2022

AMERICAN UNIVERSITY OF BEIRUT

ASSESSING THE OPERATIONAL LIMITS OF THE INTENSIFICATION OF CARBON CAPTURE BY ALKALINE SOLUTIONS

by
IBRAHIM GEORGES SALAMOUN

Approved by:

	Signature
Dr. Fouad Azizi, Associate Professor Department Chemical Engineering and Advanced Energy	Advisor
	Signature
Dr. Mahmoud Al-Hindi, Associate Professor Department Chemical Engineering and Advanced Energy	Member of Committee
	Signature
Dr. Walid Saad, Associate Professor Department Chemical Engineering and Advanced Energy	Member of Committee

Date of thesis defense: February 2, 2022

AMERICAN UNIVERSITY OF BEIRUT

THESIS RELEASE FORM

Student Name: ___Salamoun___________ Ibrahim_____________ Georges___________
Last First Middle

I authorize the American University of Beirut, to: (a) reproduce hard or electronic copies of my thesis; (b) include such copies in the archives and digital repositories of the University; and (c) make freely available such copies to third parties for research or educational purposes:

☐ As of the date of submission

☐ One year from the date of submission of my thesis.

☐ Two years from the date of submission of my thesis.

☒ Three years from the date of submission of my thesis.

Ibrahim Georges Salamoun 10-2-2022

____

Signature Date

ACKNOWLEDGEMENTS

I would like to thank and express deep gratitude and appreciation to my thesis advisor Prof. I would like to thank and express deep gratitude and appreciation to my thesis advisor Prof. Fouad Azizi for his constant help, support and guidance all throughout the past few years. Not to mention the support and assistance I was provided with from the Chemical Engineering Labs, notably Rita Khalil and Mohammad El Berjawi, and Dr. Nicolas Aramouni for assembling the entire system and developing the Lab view codes.

Special thanks to Prof. Mahmoud Al-Hindi and Prof. Walid Saad for being members of my thesis committee.

Finally, I would also like to thank my family and friends, notably my mother, father and sister, for their daily support, motivation and encouragement along the way.

ABSTRACT
OF THE THESIS OF

Ibrahim Georges Salamoun for Master of Chemical Engineering

Title: Assessing the Operational Limits of the Intensification of Carbon Capture by Alkaline Solutions

Carbon capture is one of the techniques for reducing the impact of greenhouse gas emissions on the environment. Several carbon capture methods have been developed and are constantly being improved and optimized, but the most promising appears to be that involving a chemical reaction. This study focuses on testing the limits of intensifying the chemical absorption of CO_2 into a NaOH aqueous solution. To accomplish this, various process parameters were altered including the pH of the solvent, total superficial liquid and gas velocities and the CO_2 content of the gas stream.

The efficiency of the reactor in removing carbon dioxide was determined by calculating the CO_2 removal efficiency, the specific energy consumption of the operation, and by comparing it to the physical absorption of CO_2 in water under similar hydrodynamic conditions. The removal efficiency of CO_2 was measured along the length of the reactor and was found to increase with the increase in either total superficial velocity, CO_2 concentration in the gas phase or NaOH concentration in the liquid phase. Efficiencies as high as 91.4% were recorded at the cost of 148.65 kWh/tonne-CO_2. The results were found very promising for further optimization of the process.

TABLE OF CONTENTS

ILLUSTRATIONS

Figure

TABLES

Table

ABBREVIATIONS

a	Interfacial area of contact	[m^2/m^3]
b	Screen wire diameter	[μm]
$\left(C_{CO_2}\right)^*$	Concentration of CO_2 at equilibrium with the gas phase	[$mol \cdot L^{-1}$]
D	Pipe diameter	[m]
E	Energy dissipation rate	[kW]
E_{CO2}	Energy consumption rate per unit mass of CO_2 absorbed	[kWh/tonne-CO_2]
H_{CO_2}	Henry's law constant in an electrolyte solution	[$mol \cdot bar^{-1} \cdot L^{-1}$]
k_L	Liquid side mass-transfer coefficient	[$m \cdot s^{-1}$]
L	Inter-screen spacing in the mixing section	[m]
M	Wire mesh size	[m]
Mn	Mesh number	[-]
P_{CO_2}	Partial pressure of CO_2	[atm]
Q	Volumetric flow rate	[m^3/s]
R	Gas constant	[$atm \cdot L \cdot mol^{-1} \cdot K^{-1}$]
t	Residence time	[s]
T	Temperature	[K]
U	Superficial velocity	[m/s]
V	Volume	[L]

Greek Symbols

α	Percentage open area of screen	[%]
ΔP	Pressure drop in the pipe	[Pa]
ε	Turbulent kinetic energy dissipation rate	[W/kg]
ρ	Density	[kg/m^3]
φ	Gas holdup	[%]

Subscripts

g	Gas
L	Liquid
T	Total

CHAPTER I

INTRODUCTION

Nowadays, global warming is highly endorsed by the scientific community. In 2016, the global land and ocean surface temperatures had increased compared to those recorded in the pre-industrial period (NASA, 2017). The frequency of occurrence of heat waves and extreme precipitations has been increasing over the past few years. Carbon dioxide is the highest contributor to these distresses on Earth's energy balance, also known as the greenhouse effect, and human beings are the main reason behind the exponential rise in atmospheric CO_2 levels (Intergovernmental Panel on Climate Change, 2014). The atmospheric concentration of CO_2 has been increasing at the fastest observed rate, such that 2016 was the first year where atmospheric CO_2 concentration did not fall below 400 ppm (Scripps Institution of Oceanography, 2017). At the 2015 United Nations Climate Change Conference in Paris, 190 countries agreed to lower the emissions of greenhouse gases to ensure that the global temperature increase is kept below 2 °C by the year 2100 (Anderson et al., 2016), which would require maintaining CO_2 atmospheric concentrations below 450 ppm (Intergovernmental Panel on Climate Change, 2014). According to the International Energy Agency (2015), to achieve such mitigation, the electricity and heat generation sectors need to be decarbonized, since they generate more than two-fifths of global CO_2 emissions (IEA, 2018). In 2009, Europe established a mutual policy (Directive 2009/28/EC) (European Parliament, 2009), which aims to increase renewable shares to 34% in the electricity sector and 21% in the heat sector by 2020. This would reduce the associated emissions by more than 12% (Eurostat, n.d.). However, high intermittent energy production in the electricity sector (European

Commission, 2017) will make creating a balance between generating power and the demand on it a difficult task.

Carbon dioxide capture, utilization and storage are important methods in the field of CO_2 emission control. CO_2 capture techniques are used to remove the CO_2 from gas streams (Wong & Bioletti, 2002) and can be categorized into three approaches: Pre-combustion, Oxy-Combustion and Post-combustion (Leung et al., 2014; Zhang et al., 2018). Different separation techniques can be incorporated into post-combustion carbon capture such as adsorption, absorption, chemical looping, membrane, hydrate based separation and cryogenic (Seader et al., 2010; Wang et al., 2011; Abanades et al., 2015). In utilization procedures, CO_2 is converted into more valuable products, such as methane, while in storage procedures the captured CO_2 is stored by applying different techniques (Zendehboudi et al., 2012; Zendehboudi et al., 2013).

Post-combustion CO_2 capture has proven to be the most cost-effective compared to the pre- and oxy-combustion CO_2 capture approaches (Macdowell et al., 2010). Solvent-based absorption is the most widely employed and well-known separation technique used in post-combustion CO_2 capture (Koronaki et al., 2015; Borhani et al., 2018) and is classified into three categories based on the solvents used, which are physical, chemical and chemical-physical/mixture solvents (Borhani & Wang, 2019).

In physical absorption processes, the gas absorption is achieved under high pressure conditions whereas solvent regeneration is achieved by reducing the pressure (Mumford et al., 2015). Physical absorbents, such as propylene carbonate and methanol, have greater absorption capacities compared to chemical solvents, which results in lower recirculation rates (Kidnay & Parrish, 2006). Whereas in chemical absorption (chemisorption), the reaction between the CO_2 and chemical solvents increases the rate of absorption due to two factors (Glasscock, 1991):

i. The reaction in the liquid phase lowers the equilibrium partial pressure therefore increasing the mass transfer.

ii. The reaction consumes the CO_2 at the interface thus increasing the CO_2 concentration gradient.

The main advantage of using chemical solvents, such as hydroxides and amines, is their insensitivity to acid gases partial pressure, high absorption/desorption mass transfer coefficients and high capture level of acid gases (Li & Keener, 2016; Borhani et al., 2019). Chemisorption is seen as one of the most economical means of reducing CO_2 emissions from flue gas (Yang et al., 2011). Alternatively, investigations on carbon capture using aqueous NaOH solution have been conducted over the years (Chen et al., 2014; Chiang et al., 2017; Kordylewski et al., 2013; Tavan & Hossein, 2017) and have shown significant results due to its strong reactivity with CO_2 and lower vapor pressure (Isa et al., 2018).

Chemical absorption is a multiphase reaction that has been incorporated in many gas-liquid reactors/contactors. Some of these contactors include bubble columns, packed-bed absorption columns, hollow fiber membranes, mechanically agitated vessels and rotating packed beds (Yang et al., 2011; Aroonwilas et al., 1999; Chavez & Guadarrama, 2010; Kim & Yang, 2000; Chiang et al., 2017; Lin and Kuo, 2016). Complex hydrodynamic conditions prevailing in these contactors/reactors, such as the local value of mixing intensity, bubble size distribution and gas holdup, have made it difficult to design such units without the employment of empirical knowledge and experience and pilot-scale testing (Azizi & Taweel, 2015). Studies on the absorption of CO_2 into aqueous

NaOH solutions were done on several reactors, such as packed columns (Gavini, 2017), bubble columns (Chen and Liao, 2014) and rotating packed beds (Chiang et al., 2017). These studies were conducted in an attempt to determine the mass transfer coefficient and gas liquid interfacial area using various packing material (Duss et al., 2001; Tsai and Chen, 2015; Luo et al., 2017).

Although many carbon capture techniques are viably mature to be used in the industry, they may lead to excessive costs and thus the inevitable termination of their use. Process intensification (PI) was one of the approaches that were adopted to achieve enhancements in the economy and efficiency of the industry's chemical processes, which consequently led to the development of cleaner, safer, smaller and more efficient process technologies (Reay et al., 2013; Pangarkar, 2017; Budzynski, 2017). Several studies, involving desulphurization and oxygen desorption, have shown the benefits of process intensification in enhancing the volumetric mass transfer between the liquids and gases (Al Taweel et al., 2013; Azizi & Al Taweel, 2015).

Tubular reactors equipped with static mixers, in which the flowing phases traverse the reactor co-currently in turbulence, pose as an attractive alternative to the conventional multi-phase reactors used, which include mature technologies such as amine-based absorption, aqueous ammonia-based absorption, membranes, gas hydrate formation and adsorption materials (Sabouni et al., 2014). These static mixers have been used to enhance the mass transfer performance of the contactors and mixing efficiency. In recent studies static mixing elements, such as screens or grids, have been used to repetitively superimpose an adjustable uniformly distributed turbulence field on the plug flow conditions seen in high velocity pipe flows (Ghanem et al., 2014; Thakur et al., 2003; Abou Hweij & Azizi, 2015). Using the same experimental setup as Kaady et al. (2018), a study was conducted to investigate the potential of employing screen-type static mixers to intensify the chemical absorption of CO_2 into aqueous NaOH solutions under different operating conditions, such as gas hold-up and total superficial velocities, and design configurations, and different mesh geometries and found that the efficiency increases with liquid superficial velocity and gas volume fraction to up to 98%, respectively.. In the current work, the same tubular reactor equipped with static mixers will be used to study the operational limits of the intensification of carbon capture using aqueous NaOH solutions. In particular, the effect of changing the NaOH concentration (i.e., pH of the solvent) and the CO_2 content of the gas phase will be monitored in terms of CO_2 removal efficiency. In addition, the efficiency of the contactor will also be assessed based on its energy consumption per unit mass of captured CO_2.

CHAPTER II

LITERATURE REVIEW

Three main techniques have been developed to reduce the total CO_2 emissions into the atmosphere, the first two incorporate the efficient use of energy and the transition towards cleaner forms of energy, such as renewable energy (Olajire, 2010; Yoo et al., 2013). The third method involves developing and enhancing technologies and processes to capture and sequester CO_2 (CCS). In an ideal situation, eliminating the use of fossil fuel as an energy source and transitioning to non-fossil fuel energy alternatives sounds like the best alternative, but the issue lies in not being able to meet the energy demand and disrupting the existing energy infrastructure(Olajire, 2010). Therefore, the mitigation of CO_2 by enhancing existing technologies or developing new ones for CCS remains an important task. Many researchers have aimed towards improving and developing more efficient and cost effective technologies to separate and capture CO_2 (Olajire, 2010; Samanta et al., 2012; Yang et al., 2008).

In this section, previous investigations on the chemical absorption of CO_2 in aqueous solutions and the physical absorption of CO_2 in water will be discussed and compared and recent advances in carbon capture and its utilization will be discussed.

A. Physical absorption of CO_2 into water in different reactors

Only few investigators considered the physical absorption of CO_2 in pure water without chemical reactions. Hill (2006) studied the mass transfer of CO_2 into water using a direct pH measurement technique to track the dissolution of CO_2 in water and developed a model based on temperature, aeration rate and stirring speed to evaluate the mass transfer coefficients. He also studied the effect of dissolved salts on k_La by incorporating a 2.85% NaCl solution as the solvent. Lisitsin et al. (2008) conducted studies on CO_2 desorption from pure water and calculated the mass transfer coefficient based on the difference between the bulk concentration of CO_2 and the equilibrium concentration of CO_2. Nieves-Remacha et al. (2013) explored the hydrodynamics and mass transfer of gas-liquid flow in an advanced flow reactor using carbon dioxide and water. The gas liquid mass transfer was obtained by determining the amount of CO_2 absorbed in the liquid phase by analysing extracted samples using titration with sodium hydroxide and hydrochloric acid. The experiments were performed at ambient conditions at low gas and liquid flow rates, ranging between 5.6-103 mL/min and 10-80 mL/min respectively. Their conclusion was that the bubble size distribution is directly affected by both gas and liquid flow rates and that the average bubble size decreases gradually as the liquid flow rate increases while keeping the gas flow rate constant.

Moreover, Panja and Rao (1993) investigated the absorption of CO_2 in water using a contactor with mechanical agitators and concluded that as the gas flow rate increased the k_{La} value increased as well. Thaker and Rao (2007) studied the hydrodynamics of CO_2 absorption in distilled water using a bubble column, where the feed gas was saturated with water vapour and was fed into a packed bed disperser, and the absorption efficiency was evaluated by analysing collected water samples using titration. They found that higher values for k_{La} were observed at higher gas flow rates and as the gas hold-up decreases. In another study, Evren et al. (1999) investigated the absorption of a mixture of CO_2 and air in water using a packed-bed recirculating absorption column, and observed that as the water flow rate and gas holdup increase, the k_{La} value increases. They also concluded that the temperature and gas flow rates did not affect the value of k_{La}.

Other studies considered the absorption of CO_2 in sea water with no solvents. For instance, Tokumura et al. (2007) investigated CO_2 absorption in seawater using a cylindrical bubble column by studying the effect of salinity, temperature and gas flow rates on the absorption capacity. They concluded that increasing the salinity and temperature reduced the absorption of CO_2, while increasing the gas flow rate of the pure CO_2 stream enhanced the CO_2 absorption rate. Furthermore, Chen and Vallabh (1970) studied the effect of cylindrical screen packings on the rate of mass transfer in counter-current gas-liquid bubble column, over a range of gas and liquid flow rates. Mixtures of CO_2 and air of known proportions were used, and the rate of CO_2 absorption in water was determined by a titration method. They concluded that as the gas flow rate increased, the k_{La} values increased until they reached a constant value at a certain gas flow rate and that as the mesh number (Mn) of the screens increased, the k_{La}, increased due to a decrease in bubble size.

Interest in tubular reactors equipped with static mixers for carbon capture are an attractive alternative to conventional reactors/contactors, due to their controlled hydrodynamics which enhance the mixing efficiency and mass transfer performance of the carbon capture operation (Azizi & Al Taweel, 2015). Screens are used to repeatedly overlay a consistently distributed and adjustable turbulence field on the practically plug flow conditions (Azizi & Abou Hweij, 2017; Abou Hweij & Azizi, 2015) faced in high-velocity pipe flows (Azizi & Al Taweel, 2011). These mixers were employed in similar cases to enhance mass transfer in turbulently flowing gas−liquid dispersions (Azizi & Al Taweel, 2015; Azizi & Abou Hweij, 2017; Abou Hweij & Azizi, 2015; Azizi & Al Taweel, 2011; Al Taweel et al., 2005) and liquid−liquid dispersions (Al Taweel et al., 2013; Al Taweel et al., 2007) at relatively low power consumption rate.

B. Chemical absorption using amine-based systems and carbonate-based systems

Chemisorption, or chemical absorption, is the most effective way of capturing and sequestering CO_2 from a mixture of flue gas that has a low CO_2 partial pressure (Olajire, 2010; Yoo et al., 2013). Ideally, the best candidates to be used as chemical solvents for the chemisorption of CO_2 should have fast CO_2 absorption rate, low regeneration energy requirement and degradation rate and low cost and corrosivity (Aroonwilas et al., 1999; Devries, 2014; Gabrielsen et al., 2007; Kim and Cho, 2011; Koronaki et al., 2017). These amine-based absorbents can be classified into four groups: primary, secondary, tertiary and sterically hindered amines. Primary and secondary amines react rapidly with CO_2 to form carbamate. MEA is a widely used solvent due to its low cost, high reactivity and absorption rate, which justifies it being the absorbent for carbon capture in many conducted studies and published articles (Aroonwilas et al., 1999; Devries, 2014; Gabrielsen et al., 2007; Kim and Cho, 2011; Koronaki et al., 2017; Kothandaraman et al., 2009; Kumar et al., 2014; Lin and Kuo, 2016; Spigarelli, 2013). Studies developed and validated a rate-based model for CO_2 absorption into MEA capable of predicting the profile of various process parameters, including the temperature and mole fraction as a function of length of the absorber (Koronaki et al., 2017). They also concluded the importance of the chemisorption process of CO_2, which reduces the size of the absorber and gas-liquid contactors. Other studies investigated the effect of various parameters, such as the pH, mole fraction of CO_2 in the gas mixture, gas flow rate and liquid flow rate, to determine the optimum conditions for CO_2 capture using MEA in different reactors, which include a bubble-column scrubber and packed beds (Chen et al., 2014; Kothandaraman et al., 2009; Rezazadeh et al., 2017; Thee et al., 2012). For example, Chen et al. (2014) concluded that the absorption rate in bubble columns is greatly affected by the pH and mole fraction of CO_2, such that low CO_2 concentrations in the gas phase and high pH values in the liquid phase increase the absorption rate. Lin et al. (2015) concluded that the higher the gas and liquid flow rates, the higher volumetric mass transfer coefficient. Aqueous monoethanolamine (MEA) with 30 wt% is a great candidate to capture CO2, in terms of low operating cost and high absorption capacity (Zhou et al. 2012). MEA-methanol is considered as a better absorbent than aqueous MEA because of its lower regeneration temperature (Jie et al. 2016) However, the downside of using MEA as the solvent choice for chemisorption of CO_2 is that it degrades easily, it's highly corrosive and regenerating it requires a lot of energy (Isa et al., 2018; Kim et al., 2013; Saeed et al., 2018). A better solvent than MEA is DEA, a secondary amine, which is less corrosive, more stable and has a slower reaction rate. (Isa et al., 2018; MacDowell et al., 2010). To compensate for these issues, ionized liquids are being introduced as the better absorbents that could overcome some disadvantages arising with the alkaline amines (Akbari and Valeh-e-Sheyda 2019).

As for tertiary amines, the carbamation reaction does not take place due to the absence of a hydrogen atom attached to the nitrogen atom. Instead, a base-catalysed hydrolysis reaction takes place producing bicarbonate, HCO_3^-. This hydrolysis reaction generates less heat compared to the carbamation reaction resulting in a lower solvent regeneration cost (Kim et al., 2013). MDEA, a hybrid of MEA and DEA which happens to be a tertiary amine, although it has a higher degradation resistance and improved CO_2 loading capacity, corrodes when exposed to oxygen (Isa et al., 2018; Mandal et al., 2001). Some researchers incorporated mixed amines as chemical absorbents in order to get the mentioned desirable qualities of individual amines(Yang et al., 2008). Chen and Liao (2014) investigated using the blend DEEA (N,N-diethylethanolamine)/EEA (ethylethanolamine) as a chemical solvent for the chemisorption of CO_2 and found that using this mixed solvent proved to have an efficiency in the range 29-98.66% and a mass transfer rate in the range 0.0728-0.08395 s^{-1} along the various operating conditions. MEA is facing serious issues, although proven to be the most cost efficient like a larger equipped requirement, corrosive issues, and lower CO_2 loading capacity at certain temperatures. As compensation of this, ionized liquids are being introduced as the outstanding absorbents by overcoming some disadvantages arising with the alkaline amines (Akbari and Valeh-e-Sheyda 2019). The use of sterically hindered amines (such as 2-amino-2-methyl-1-propanol) as CO_2 absorbents has also been reported in the literature and has been proven to be less of a viable candidate to be used as a solvent due to its molecular structure, which results in the formation of an unstable carbmate that can react with water to form free amines or bicarbonates. Although this reduces the regeneration temperature, but it makes the reaction slower (Kim et al., 2013; Olajire, 2010; Vaidya and Kenig, 2007).

Potassium carbonate (K_2CO_3) has been investigated as a solvent for carbon capture due to its low cost, enthalpy requirements and toxicity and its high degradation resistance, but its only disadvantage is its poor kinetics, which results in the need for large absorption columns (Isa et al., 2018). Using K_2CO_3 as a solvent for the chemisorption of CO_2 reduces the energy consumption of the regeneration process by 37% (Thee et al., 2012). Incorporating different promoters could overcome the poor kinetics of using K_2CO_3 as a solvent (Hu et al., 2016; Hu et al., 2017), such as inorganic promoters like arsenite (Phan et al., 2015; Shen et al., 2013), organic promoters like MEA (Thee et al., 2012) or enzymatic based promoters like carbonic anhydrase (Thee et al., 2015). Using these promoters improves the reaction kinetics and reduces the energy consumption needed for regeneration (Hu et al., 2016).

Using the same carbon capture system and solvent as the one used in this study, Kaady et al. (2018) previously studied the effect of different operational conditions (total superficial velocity and gas hold-up (%)) and static screens' geometries on the volumetric mass transfer coefficient, removal efficiency of CO_2 and specific energy consumption. It was concluded that the volumetric mass transfer coefficients and efficiencies increased with liquid superficial velocity and gas hold-up to $1.3563 s^{-1}$ and 98%, respectively and that screens having smaller open area (greater Mn) yielded the highest k_La values, even higher than other gas/liquid contactors that incorporate NaOH as their solvent for the chemisorption of CO_2, like bubble columns, rotating packed beds and packed beds.

C. Chemical absorption of CO_2 into NaOH in different reactors

Many investigations have been conducted on the capture of CO_2 using aqueous NaOH solution (Chen et al., 2014; Chiang et al., 2017; Fleischer et al., 1996; Guo et al., 2011; Kordylewski et al., 2013; Lin et al., 2003; Luo et al., 2012b; Niu et al., 2009; Tavan and Hossein, 2017; Kaady et al., 2018). The reaction of CO_2 with alkaline solvents (such as aqueous NaOH) is considered less complex than the reaction of CO_2 with alkanol amines, which results in the formation of carbamate and bicarbonate (Couchaux et al., 2014; Krauβ and Rzehak, 2017; Vaidya and Kenig, 2007; Versteeg et al., 1996). Additionally, NaOH has a lower vapour pressure and a strong reactivity with CO_2 (Isa et al., 2018). Studies conducted by Yoo et al. (2013), Aroonwilas (2001), Devries (2014) and Gavini (2017) showed that NaOH has a higher absorption capacity than MEA, but using it as an absorbent for CO_2 has proven to be a costly technology (Isa et al., 2018).

Regenerating NaOH is not an easy operation and requires a lot of energy due to the formation of Na_2CO_3, a thermally stable compound, which decomposes into Na_2O. Na_2O decomposes at very high temperature to form NaOH (Yoo et al., 2013).

Many reactors incorporated NaOH solutions as the solvent for the chemisorption of CO_2 such as: bubble columns (Chen and Liao, 2014), packed columns (Aroonwilas, 2001; Aroonwilas et al., 1999; Gavini, 2017), rotating packed bed, RPB, (Chiang et al., 2017; Lin et al., 2003; Lin and Kuo, 2016; Tsai and Chen, 2015) and spray dryers (Guo et al., 2011; Niu et al., 2009; Tavan and Hossein, 2017). Studies conducted on CO_2 absorption into aqueous NaOH were mainly carried out to determine the mass transfer characteristics of gas/liquid reactors or the influence of different packing materials. Many studies used NaOH as the solvent for the chemisorption of CO_2 to determine the effective gas-liquid interfacial area as function of different parameters, such as packing elements, surface tension, liquid flow rate and gas flow rate (Luo et al., 2017; Duss et al., 2001; Skoczylas and Majewski, 1991; Tsai and Chen, 2015; Vàzquez et al., 2000; Weiland et al., 1993; Yoshida and Miura, 1963).

Bubble columns were used for CO_2 absorption into aqueous NaOH solution, and results show that the removal efficiency and K_{Ga} varied between 30-98% and 0.018-0.058 s^{-1} respectively (Chen et al., 2014). Inserting multiple screens along a bubble column can greatly improve the performance of the contactor by decreasing the Sauter mean diameter of the bubbles, thus increasing the interfacial area of contact between both gaseous and liquid phases and enhancing the mass transfer and chemical reaction rate (Jain et al., 2015). Other studies were conducted to investigate the effect of various operating and design conditions on the mass-transfer coefficient in packed beds with different packing types. For example, Gavini (2018) studied the absorption of CO_2 into NaOH in a randomly packed column and discovered that the overall gas mass transfer coefficient increased from 37.2 $mol.m^{-3}.min^{-1}$ to 45.67$mol.m^{-3}.min^{-1}$ when the concentration of NaOH increased from 0.003 M to 0.01 M due to the rapid reaction occurring. Although these studies are conducted on the industrial scale, a very important parameter that influences the economic feasibility of a process, such as the energy consumption of the process, was not directly determined.

Rotating packed beds (RPB) have proven to be far more superior to other reactor, resulting in high mass transfer coefficients and increased CO_2 removal efficiencies of 95.6% (Pei et al., 2017). This success can be attributed to the replacement of the gravity force in packed columns with a centrifugal force in rotating packed beds and the reduction in size and capital, which instigated great effort in the field of process intensification (Tsai and Chen, 2015). Lin and Kuo (2016) investigated the CO_2 absorption in a RPB with two different design packing: blade and structured packing. It was determined that under the same operating conditions, the blade packing generated a higher CO_2 absorption rate than structured packing and that the higher the gas and liquid flow rates, the higher the volumetric mass transfer coefficient. Lin et al. (2003) investigated the absorption of CO_2 into NaOH in a cross-flow rotating packed bed and concluded that an increase in the liquid flow rate and NaOH concentrations lead to an increase in the K_Ga values. In addition to that, K_Ga values in a cross-flow RPB reached 1.4 s^{-1} and were higher than that in a countercurrent-flow RPB for 10%v CO_2 concentration and 1 M NaOH (Lin et al., 2003). Chiang et al. (2017) investigated the effect of adding glycerol to the aqueous NaOH solution in a rotating packed bed and found that it increased the CO_2 absorption efficiency to more than 90%, and the resulting heat capacity of the aqueous NaOH solution decreased, thus lowering the heating requirement to generate the solvent.

Studies conducted on spray dryers (Niu et al., 2009; Tavan and Hossein, 2017) aimed to determine the effect of the concentration and flow rates of both CO_2 and NaOH on the removal efficiency. It was found that in order to achieve a higher CO_2 removal efficiency, the equivalence ratio of NaOH to CO_2 flow rate should be larger than 4.43.

Therefore, the issue of developing cheaper and more efficient carbon capture technologies arises and in the process of developing them one must evaluate the volumetric mass transfer coefficient, removal efficiency and energy requirement.

D. Recent advances in carbon capture technologies

The mass transfer process intensification has potential to significantly reduce capital cost (Wang et al., 2015). Many process intensification technologies have been suggested for the absorption of CO_2, which include hollow fiber membrane contactors (HFMC), the rotating packed beds (RPB), micro-channel reactors and three-phase fluidized beds (Tay et al., 2019). In HFMC absorption, the membrane acts as a separator between the gas and the liquid phase and based on the properties of the solvent, the selectivity for the gas is determined. The advantages of this technology include: large surface area, small volume and light weight and prevents issues such as foaming, channelling and flooding by providing an independent flow pathway for both gas and liquid streams (Zhang, 2014). The disadvantages of this technology are the low heat transfer coefficient and the limitations of the operating pressure and that of solvent viscosity. The capital and maintenance cost of HFMC is relatively high due to the costly pre-treatment process of the membrane, which is done to avoid a decrease in the absorption of CO_2 (Ilea et al., 2020).

Micro-channel reactors are far more superior to other carbon capture process intensification technologies that is because of their much higher mass and heat transfer coefficients. The mass transfer coefficient in these reactors can be up to 100 times greater than that of conventional packed bed columns. The advantages of the micro-channel reactor include minimum energy requirement and high chemical stability. The possible challenge of using this reactor for carbon capture is the huge volume of flue gas that needs to be treated (Tay et al., 2019).

The three-phase fluidized beds are used in the chemical, petrochemical, and biochemical industries to carry out a variety of chemical reactions. The gas-solid-liquid three-phase fluidized absorber is an innovative process intensification technology in which the bed is composed of low density packing (inert solid hollow spherical balls) fluidized by a stream of gas, that is rich in CO_2, counter currently flowing with the liquid stream (Dragan, 2016). The solid phase acts as an agitator, intensively mixing in the column inducing high turbulence vortices and therefore enhancing the mass transfer coefficient compared to that in conventional fixed packed beds. This contactor design has many advantages: low pressure drop in the column, high interfacial contact area, and its ability to continuously process large volumes of gases. These attributes make three phase fluidized bed absorbers suitable for air pollution control and industrial scale operations (Ilea et al., 2020).

CHAPTER III

EXPERIMENTAL SECTION

In order to determine the absorption of CO_2 into aqueous NaOH solution, a plug flow reactor with screen-type static mixers was used. In this section, a description of the chemisorption reaction and the employed experimental setup will be done followed by the different parameters investigated. Then the method of analysis will be explained accompanied with the different equations required to calculate the volumetric mass transfer coefficient, efficiency and power consumption in continuously flowing reactors.

A. Reaction of CO_2 with aqueous NaOH

The mechanism of CO_2 absorption in an NaOH aqueous solution (Krauβ and Rzehak, 2017; Niu et al., 2009; Wang et al., 2010) can be explained as follows:

Firstly, NaOH is almost completely dissolved in pure water and dissociates into Na^+ and OH^- because NaOH is strongly alkaline. Secondly, when gaseous CO_2 is fed into the NaOH solution to be absorbed, CO_2 is physically absorbed (Darmana et al., 2007) to aqueous CO_2, according to Reaction (1).

$$CO_{2_{(g)}} \rightarrow CO_{2_{(aq)}} \qquad [[1]$$

The dissolved CO_2 then gets chemically absorbed by hydroxide ions in the solution, forming both bicarbonate, HCO_3^- and carbonate CO_3^{2-} according to the following Reaction (2) and (3):

$$CO_{2_{(aq)}} + \ OH_{(aq)}{}^{-} \leftrightarrow \ HCO_{3(aq)}^{-} \qquad 2[2]$$

$$HCO_{3(aq)}^{-} + OH_{(aq)}{}^{-} \leftrightarrow CO_{3(aq)}^{2-} + H_2O_{(l)} \quad [[3]$$

Although Reaction (2) is a second-order reaction, it can be considered a pseudo first-order reaction since the CO_2 concentration is kept constant in this study for each experimental run (Yoo et al., 2013). Reaction (2) and (3) are reversible fast reactions at high pH range (Fleischer et al., 1996). Reaction (3) takes place immediately after Reaction (2) (Guo et al., 2011). Aqueous CO_2 does not exist in the solution during the overall reaction due to its immediate reaction and consumption via Reactions (2) and (3) with OH^- after its formation. Due to the high concentration of NaOH maintained in the liquid phase, Reaction (3) is the dominant reaction, which further increases the CO_3^{2-} concentration compared to that of HCO_3^- (Fleischer et al., 1996). In addition, OH^- is rapidly decreased through Reactions (2) and (3). Although Na_2CO_3 is produced, it exists as dissociated Na^+ and CO_3^{2-} in the absorbent. Therefore, while pH is rapidly decreased during the initial period of the reaction, the CO_3^{2-} concentration increases. Based on these phenomena, the net reaction carried out during the initial time (or range) of overall CO_2 absorption reaction is expressed as listed in Reaction (4).

$$CO_{2_{(aq)}} + 2OH_{(aq)}{}^{-} \rightarrow CO_{3(aq)}^{2-} + H_2O_{(l)} \quad [[4]$$

Subsequently, as CO_2 is continuously fed into the NaOH solution in the reactor/contactor during the reaction, CO_2 is continuously absorbed, which leads to OH^- depletion and CO_3^{2-} accumulation through Reaction (2) and the forward direction of Reaction (3). However, the CO_3^{2-} concentration increase favors the backward reaction of (3), thus accelerating the forward direction of Reaction (2). Therefore, the HCO^-_3 concentration and pH decrease in this range. The net reaction in this second range of the overall absorption reaction is expressed as Reaction (5).

$$Na_2CO_{3(aq)} + CO_{2(g)} + H_2O_{(l)} \rightarrow 2NaHCO_{3(aq)} \quad [[5]$$

After Reaction (5) is completed at equilibrium, a small amount of CO_2 may be additionally absorbed to compensate for the shortage of physically unabsorbed CO_2 in water during the reaction. If NaOH is the limiting reactant, the overall CO_2 absorption reaction with NaOH in aqueous solution can be summarized as Reaction (6), which is the net reaction of Reactions (4) and (5).

$$NaOH_{(aq)} + CO_{2\,(g)} \rightarrow NaHCO_{3(aq)} \quad [[6]$$

B. Experimental Setup

In this study, a tubular plug flow reactor equipped with screen-type static mixers was used to quantify the volumetric mass transfer coefficient, power consumption, and efficiency under different hydrodynamic conditions, gas stream CO_2 compositions and liquid stream's pH values. Figure 1 (Kaady et al., 2018) represents a scheme of the continuous flow experimental setup used. A 500L polyethylene tank was used to store reverse osmosis (RO) water and a single stage centrifugal pump (Pedrollo®, model AL-RED 135m) was used to pump the RO water into the gas-liquid contactor. A 250 L tank was used to store a high concentration NaOH stock solution, which was prepared by dissolving NaOH pellets of purity >99.15% (Formosa Plastics) in RO water. This stock solution was pumped into the liquid stream before entering the gas-liquid contactor using a dosing pump (Prominent, model CONCEPT PLUS/PVT, Teflon). The dosing was conducted and the pumping rate was changed to vary the pH of the aqueous phase, for the runs involving the use of a NaOH aqueous solution as a solvent for the chemisorption of CO_2 to a pH value of 12 ± 0.1 for the first 12 runs and 12.3 ± 0.1 for the other 12 runs, and was turned off for the 12 runs involving the use of pure RO water. The overall liquid phase flow rate (aqueous NaOH and RO water streams) was then measured using a paddle flow meter (Omega engineering, FP-90 Series) and typically varied from 23 to 49 L/min, which corresponds to liquid phase superficial velocities, U_L, ranging from 0.8 to 1.7 m/s and a pipe Reynolds number (based on total velocity) ranging from 24,830.94 to 50,000. To simulate different flue gases emitted in the industries, a 15%, 23 %, and 30%v/v CO_2/air gas stream was used throughout the experiments. Pure CO_2 stream was mixed with a compressed air stream (both flow rates were controlled using Omega Engineering, FMA-series mass flow controllers to generate gas streams of different carbon dioxide compositions) before it was injected at the bottom of the reactor/contactor where it enters it co-currently with the aqueous NaOH liquid stream or pure RO water. The total gas flow rate ranged from 6 L/min to 11 L/min in order to attain gas volume fractions of around 20% for the different liquid flow rates.

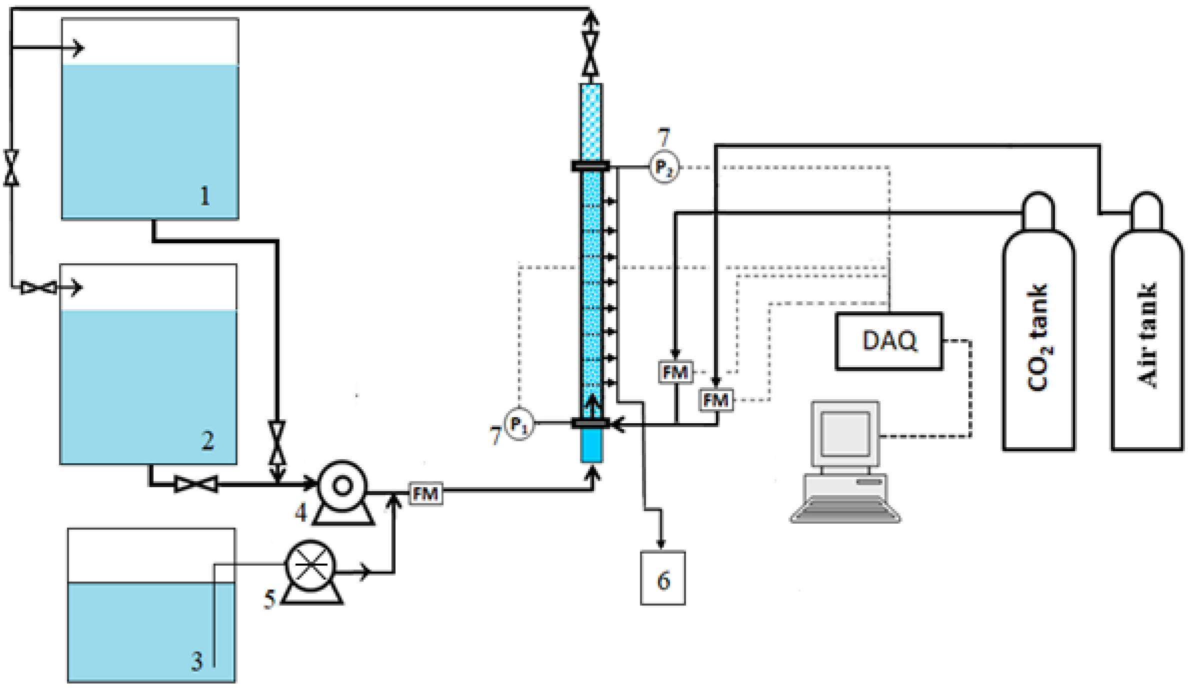

Figure 1 Schematic Representation of the experimental setup (1): supply tank (2): drain tank (3):NaOH tank (4):centrifugal pump (5): dosing pump (6): samples extracted for analysis (7): pressure sensors.

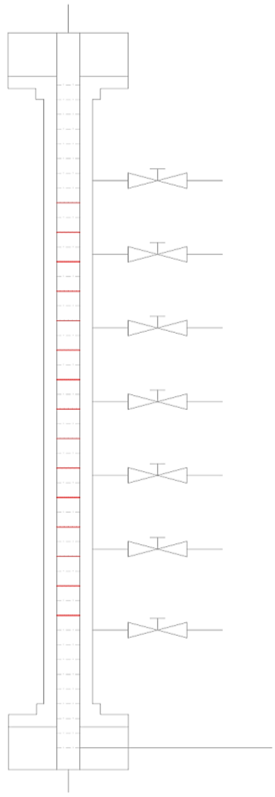

Figure 2 Reactor Internals (red lines indicating the location of the inserted screens in the column)

Gas-liquid contacting took place in a 900 mm pipe, which was fixed vertically ensuring that all multiphase radial and temporal nonuniformities caused by gravity are eliminated. In the mixing section, commercially available stainless steel (type 304) woven meshes (Ferrier Wire, Toronto, Canada) were inserted to act as static mixers. The screens used had a mesh number (Mn) of 80 and were inserted 40 mm apart in order to better disperse the gas-liquid flow (Al Taweel et al., 2007, 2005; Munter, 2010; Turunen and Haario, 1995) and intensify the mass-transfer-limited reaction (Al Taweel et al., 2013). Their characteristics are given in Table 1. Plexiglas cylindrical spacers, 20 mm in length and having an ID of 25 mm, were used and were tightly inserted in a clear PVC pipe (48 mm OD and 40.9 mm ID) in order to ensure the screens are held tight in place perpendicularly, while the streams flow co-currently through the reactor across the screens. This configuration insured immobilized the spacers while maintaining an effective flow diameter of 25 mm.

The plain weave wire gauzes that were used are characterized by their mesh number, *Mn*, which is the number of openings in one inch, the wire diameter, *b*, and the mesh size, *M*, which is the center-to-center distance between two adjacent wires. The open area of the screen can be deduced from the mesh size, *M*, and wire size, *b*, according to Equation (7). Figure 3 Screen-type static mixer3 shows a sketch of a screen element and highlights its various geometric/design parameters.

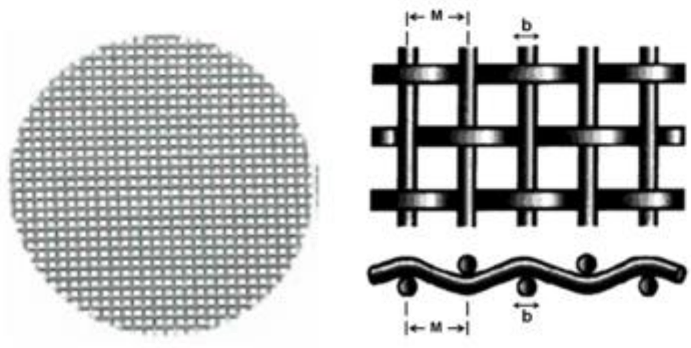

Figure 3 Screen-type static mixer

$$\alpha = \left(\frac{M-b}{M}\right)^2 \times 100 \qquad [7]$$

Table 1 Characteristics of the investigated stainless-steel plain weave wire meshes

Mesh Number, Mn	**Wire Size, b (μm)**	**Mesh size, M (μm)**	**Open Area, α (%)**
80	139.7	317.5	31.36

Seven sampling ports were provided along the reactor and were placed 10 cm apart. At each sampling port, the spacer had a 2 mm deep groove around its circumference and four 2-mm holes were drilled at 90° angles for withdrawing liquid samples and ensuring a more representative sample composition.

Both pressures at the inlet and the outlet of the reactor were measured using pressure transducers with a response time less than 0.01 s (Omega Engineering, PX-303 Series). All sensors were controlled using a National Instruments data acquisition board (National Instrument, model NI USB - 6212) and a specially developed LabVIEW program. Although the setup can operate in the recycle mode, all of the reported experiments in this investigation were performed using a once-through approach.

In this study, various operating conditions were varied in order to investigate the potential of intensifying the chemical absorption of CO_2 by screen-type into aqueous NaOH solutions. These conditions include varying the total velocity (1, 1,3, 1.6 and 2 m/s), pH of the liquid stream (12, 12.3 and pure RO water), and the %v/v CO_2/air of the gas stream (15%, 23% and 30%) and are summarized in Table 2.

Table 2 Operating Conditions

Condition	**Value**
Pipe diameter (mm)	25
Number of screen elements	15
Inter screen spacing (mm)	40
Screen open area (%)	31.36
Liquid superficial velocity (m/s)	0.8 to 1.6
Gas velocity (m/s)	0.2 to 0.4
Total velocity (m/s)	1 – 2
Dispersed phase holdup (%)	20

Pipe Reynolds number (based on total velocity)	25000 – 50000
Residence time (s)	0.39 – 0.78
pH	11.9-12.4
%v/v CO_2/air gas stream (%)	15-30

C. Method of Analysis

The performance of the reactor was evaluated based on the CO_2 removal efficiency and the energy required to perform the operation.

1. CO_2 Removal Efficiency

a. <u>Concentration of the reacted CO_2 in the liquid phase</u>

The carbonate content of the 7 samples extracted from the reactor/contactor, which corresponds to the CO_2 transformed and reacted from the gaseous phase to the liquid phase, were measured by titrating them using duplicate measurements with HCl and using two color indicators (phenolphthalein and methyl orange) according to Warder and Winkler method. This helps in determining the concentration of hydroxide and carbonate ions and is adapted from Crossno et al. (1996). Titration to the first equivalence point converts all NaOH and CO_3^{2-} found in the sample into bicarbonate, HCO_3^-, and titration to the second equivalence point converts all HCO_3^- into carbonic acid, H_2CO_3 (Crossno et al., 1996). A control sample, referred to as sample “0”, was taken before gas injection, for each experiment, to measure the carbonate concentration in the aqueous phase before the injection of any gas was initiated. In the case of the runs involving the use of an aqueous NaOH liquid stream as a solvent for the chemisorption of CO_2 (dosing the liquid stream with NaOH stock solution before passing through the contactor), 50 mL samples were extracted from the 7 sampling ports from which 10 mL samples were extracted and titrated twice immediately after measuring their temperatures and pH values. As for the runs involving the use of a pure RO water stream as the solvent, 20 mL samples were extracted from the 7 sampling ports which were immediately added to sterile testing cups containing 20 mL of NaOH solution with a concentration of 0.1 M. These samples were titrated twice after measuring their temperature and pH values.

b. Evaluating the CO_2 removal efficiency (%)

CO_2 removal efficiency is used as a direct index of the efficiency of the absorption process. In the case of CO_2 absorption into the solvent, the removal efficiency is reported as:

$$E\ (\%) = \frac{n(CO_3^{2-})_{formed}}{n\ (CO_2)_{injected}}\ x\ 100 \qquad [8]$$

Where, E = absorption efficiency, %

$n(CO_3^{2-})_{formed}$ = molar flow rate of the carbonate formed as a result of the chemical reaction at each sampling point, mol/min;

$n\ (CO_2)_{injected}$ = molar flow rate of CO_2 injected into the system, mol/min;

CO_2 removal efficiency is used to evaluate the overall efficacy of the CO_2 absorption for different operating conditions and to track the efficiency of each experimental condition with respect to time.

2. *Power Consumption*

Power consumption is one of the most fundamental design criteria for any reactor/contactor since it determines its economic desirability. It depends on pressure drop and the total superficial velocity. The energy input into a gas-liquid contactor can be described in multiple ways. For instance, it could be reported as the amount of energy supplied per unit time, *E*, as shown in Equation (9), or the amount of energy supplied per unit time and unit mass, ε , as shown in Equation (10) (Azizi and Al Taweel, 2015).

$$E = \Delta P.(\, Q_G + Q_L) \qquad [9]$$

$$\varepsilon = \frac{Q_L \Delta P}{\rho_L V_L} = \frac{U_L \Delta P}{\rho_L L(1-\phi)} \qquad [10]$$

Both Equations (8) and (9) are used to calculate the energy requirements of gas-liquid contactors. However in order to obtain reasonable values for the energy requirements, residence time requirements should be factored in order to assess the actual power consumption. Therefore, another approach has been proposed which better reflects the energy input, as it takes into account the residence time that is required in the contactor (Koglin et al., 1981; Al Taweel et al., 2007). The energy consumption, E_{CO2} (KW.h/tonne CO_2), which is the power needed to absorb a unit mass of aborbed CO_2 and can be calculated from the developed relation expressed in Equation (11).

$$E_{CO2} = \frac{\Delta P.(Q_G + Q_L)}{\Delta C_{CO2}.Q_G.M_{CO_2}} \qquad [11]$$

Where, E_{CO2} = energy consumption per unit mass of flowing CO_2, KW.h/tonne CO_2;

ΔP = pressure difference between the inlet and outlet, Pa;

Q_G = gas flow rate, m^3/s;

Q_L = liquid flow rate, m^3/s;

ΔC_{CO2}= CO_2 concentration difference between inlet and outlet, mol.L^{-1};

M_{CO_2} = molar mass of CO_2, tonne CO_2.mol^{-1};

Equation (11) shows that the energy consumption per unit mass of absorbed CO_2 is greatly affected by the pressure drop and the concentration gradient of CO_2 in the gas phase (difference between inlet and outlet). Thus keeping track of the decay in CO_2 concentration in the gas phase and the pressure drop are important design criteria for a tubular reactor equipped with static mixers. In this study, the pressure drop due to the screens and the high superficial velocities, which increase skin friction at the pipe wall, are expected to be the dominant ones due to the turbulent flow conditions encountered in this system. E_{co2} is also affected by the amount of absorbed CO_2, such that as the difference between the inlet and outlet CO_2 concentrations increases, the power consumption decreases. This implies that the higher the efficiency of absorption of CO_2 is, the lower the energy demand.

CHAPTER IV
RESULTS AND DISCUSSION

A. CO_2 Removal Efficiency

In order to track the efficiency of the chemisorption process in the tubular reactor/contactor, the CO_2 removal efficiency is tracked by collecting samples along the length of the column. This allows the temporal tracking of the evolution of the removal efficiency of CO_2 through the column. In this section, the effect of liquid flow rate, concentration of CO_2 in the gas phase (% v/v CO_2) and concentration of NaOH in the liquid phase (pH of liquid phase) on the removal efficiency of CO_2 were studied.

Results show that for the same experimental conditions (same gas gold-up, mesh geometry, concentration of CO_2, and pH) as the total superficial velocity increases, the efficiency of removal of CO_2 increases from a 56.48% at U_t= 1 m.s-1 to a 90.14% at Ut = 2 m.s -1, based on the analysis of the 7th sample collected from the top of the column.

In this section the effect of varying the operating and design conditions will be presented: total superficial velocity, solvent concentration (pH value of liquid phase) and CO_2 volume content in the gas phase.

1. *Effect of total superficial velocity*

According to Al Taweel et al. (2005), the total superficial velocity is a vital parameter in a co-current gas-liquid contactor/reactor, as it determines the residence time in the contactor t_{res}, intensity of the turbulence and the energy consumption. Therefore, the higher the velocity, the lower the residence time but the higher the turbulence and energy demand of the system. The turbulence downstream of the screen causes the gaseous bubbles to become more dispersed and induces bubble breakage. This phenomenon causes an increase in interfacial area of contact between the gas and liquid phases, thus increasing the rate of mass transfer (Al Taweel et al., 2005; Azizi and Al Taweel, 2015).

Figure 4 presents the CO_2 removal efficiency as a function of residence time in the reactor. As can be seen, the efficiency of removal of CO_2 increases at a faster rate as U_t increases (the slope of the trend lines increases as U_t increases). The advantage of tracking the efficiency of removal at each set of parameters is to explore the possibility of a reduction in current reactor length in order to reduce operating costs (reduced pressure drop which reduces the energy consumption) and capital costs (maintenance costs of shorter column are less).

According to Figure 4, at a pH=12.3 and 30% v/v CO_2, for U_t = 1 $m.s^{-1}$, the removal efficiency increases to a maximum of 57.4 % at a height of 68 cm after 0.68 s of residence time in the reactor. Increasing the total superficial velocity to U_t = 1.6 $m.s^{-1}$, the removal efficiency increases to 80.9% at a height of 58cm after 0.3625 s. At a total superficial velocity of U_t = 2 $m.s^{-1}$, the removal efficiency increases to 91.45% at a height of 68 cm after 0.34 s.

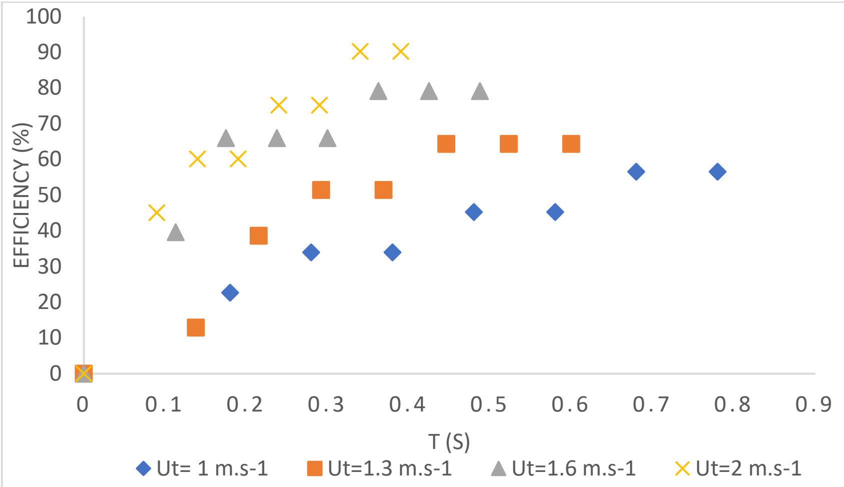

Figure 4 The effect of the total superficial velocity Ut ($m.s^{-1}$) on the efficiency of removal of CO_2 (%) as a function of the residence time at pH= 12.3 and % v/v CO_2 = 30%

It can be clearly discerned from Figure 4 that as the total superficial velocity increases, the CO_2 removal efficiency increases due to the increased turbulence. As the turbulent multiphase flow passes through these mixers bubble breakage becomes dominant and is further enhanced by the very high energy dissipation levels in the short distance downstream of the screen, leading to a larger interfacial area between the phases. Therefore, the overall removal efficiency increases as the total superficial velocity increases, which is in alignment with various studies (Niu et al. (2009), Guo et al. (2011) and Kaady et al. (2018)).

2. *Effect of the pH of the solvent*

The effect of varying the initial concentration of the solvent (pH) on the removal efficiency is an important parameter to investigate as it allows optimizing for the amount of used NaOH. Figure 5 (A) and 6 (A) display the decay of the concentration of OH^- ions in the liquid phase as a function of residence time at 2 different pH measurements (around 12 and 12.3). Figure 5 (B) and 6 (B) display the decay of the concentration of CO_2 in the gas phase as a function of the residence time. Figure 5 (C) and 6 (C) display the evolution of the concentration of carbonates in the liquid phase as a function of residence time for two different pH levels. The reason for monitoring the parameters shown in Figures 5 (30%v/v CO_2, U_t = 1.3 $m.s^{-1}$) and 6 (30%v/v CO_2, U_t = 2 $m.s^{-1}$) is to be able to:

1. Identify the direct impact of the concentration of the solvent (NaOH aqueous solution) on the evolution/decay of ionic and molecular species in the liquid and gas phase respectively, and thus identifying its impact on the absorption rate and the volumetric mass transfer coefficient.
2. Compare the findings of this study to other studies.

The rate of consumption of OH^- ions in the liquid phase is the same when the initial pH was around 12 and 12.3, as seen in Figures 5 A, 6 A and 7. According to Yoo et al. (2013), upon injecting CO_2 into the contactor, Reaction (4) prevails. Reaction (4) is a first-order reaction directly dependent on the OH^- concentration, proving that as the initial concentration of NaOH increases, the absorption rate of CO_2 increases as well, thus increasing the CO_2 removal efficiency as seen in Figure 7. Liquid stream exiting the column is always greater than 12. This proposes the possibility of recycling the solvent after exiting the reactor, and pumping it back into the column for further CO_2 removal from the gas stream. Recycling the liquid stream exiting the column reduces the amount of solvent used, thus reducing waste generation, and relieves the system from the energy consumption of the dosing pumps used to inject the solvent into the liquid stream and therefore reduces the overall cost of the carbon capture process.

In Figures 5 B and 6 B, the rate of decay of CO_2 concentration in the gas phase is slower when the initial pH was around 12 compared to that when the initial pH was around 12.3, and both curves plateau towards the end of the experiments. This further proves the effect of the NaOH concentration in the liquid phase, such that the higher the concentration of OH^- ions in the liquid stream the higher the rate of absorption of CO_2 increases.

As for Figures 5 C and 6 C, the rate of evolution of carbonates concentration in the liquid phase is higher when the initial pH was around 12.3 compared to that when the initial pH was around 12, and both curves plateau towards the end of the reactor. This shows that the higher the concentration of NaOH in the liquid phase, the higher the absorption capacity of the solvent.

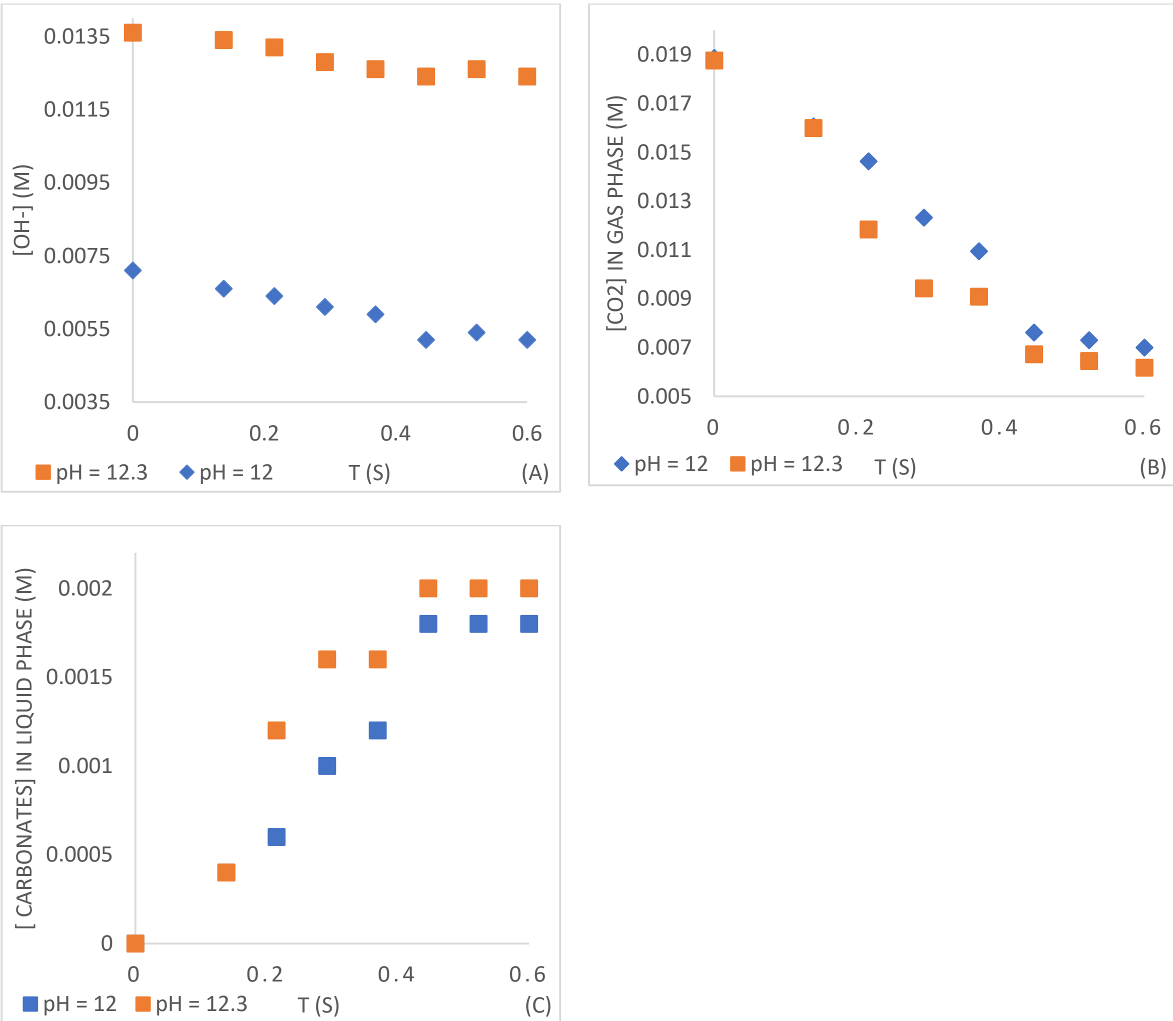

Figure 5 The variation of the concentration of OH^-(A), concentration of CO_2 in the gas phase (B) and concentration of carbonates in the liquid phase (C) as a function of residence time (s) at %v/v CO_2 = 30%, U_t = 1.3 m.s-1and pH = 12 and 12.3.

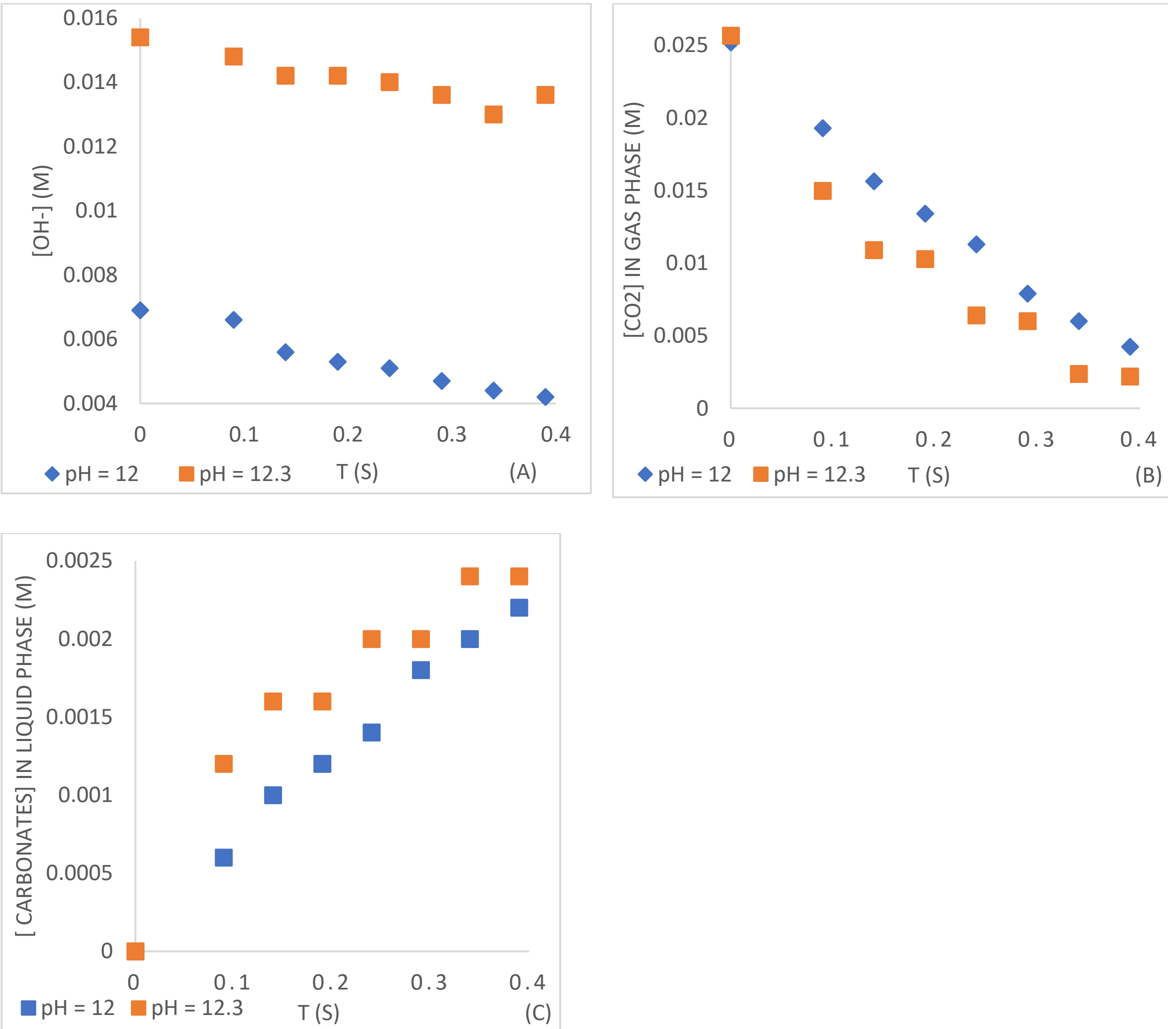

Figure 6 The variation of the concentration of OH-(A) and concentration of CO_2 in the gas phase (B) and concentration of carbonates in the liquid phase (C) as a function of residence time (s) at %v/v CO_2 = 30%, Ut = 2 $m.s^{-1}$and pH = 12 and 12.3.

The effect of the concentration of the solvent (pH) on the efficiency of removal of CO_2 are presented in Figures 7 and 8. It can be clearly observed that an increase in the concentration of the solvent, increases the removal efficiency. In Figure 7 (A), at U_t = 1 $m.s^{-1}$ and 15% v/v CO_2, at a pH = 12 the removal efficiency increases to a maximum value of 46.8% at a height of 78 cm and 0.78 s whereas at a pH= 12.3, the removal efficiency increases to a maximum of 54.22% at the outlet. Using a liquid phase with a higher concentration of NaOH for the same total superficial velocity and gas stream CO_2 composition achieves a higher removal efficiency of CO_2 and holds the possibility of further reducing the length of the reactor and even recycling the solvent for another run, thus using less solvent and reducing the cost of the carbon capture process. When comparing the removal efficiency of CO_2 using NaOH aqueous solution as the solvent with the removal efficiency of CO_2 using RO water as the solvent, the superiority of chemical absorption in carbon capture over that of physical absorption can be observed. The removal efficiency of CO_2 using a gas stream of 15% v/v CO_2 at a total superficial velocity of 1 $m.s^{-1}$ using a solvent of pH = 12 is around 16 times greater than the removal efficiency using RO water as the solvent under the same operating conditions. The removal efficiency of CO_2 using a gas stream of 30% v/v CO_2 at a total superficial velocity of 2 $m.s^{-1}$ using a solvent of pH = 12.3 is around 30 times greater than the removal efficiency using RO water as the solvent under the same operating conditions.

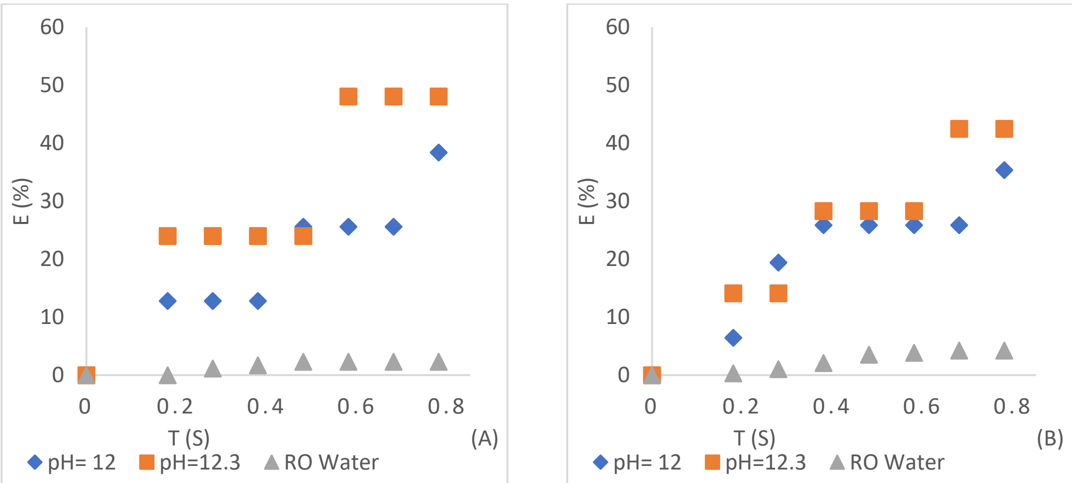

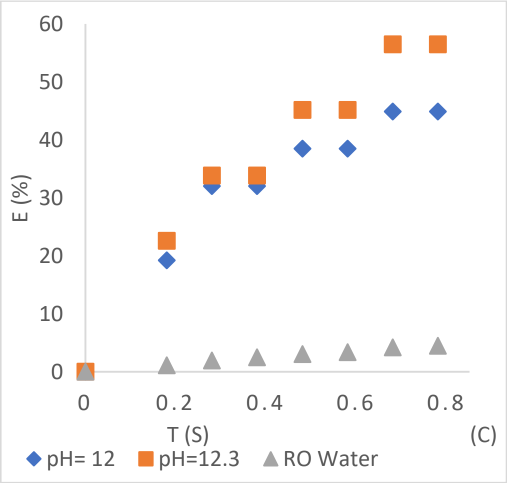

Figure 7 The effect of the concentration of NaOH (pH) on the removal efficiency E of CO_2 (%) as a function of residence time tres (s) at Ut = 1 $m.s^{-1}$ and: (A) 15 % v/v CO_2 , (B) 23 % v/v CO_2 and (C) 30 % v/v CO_2

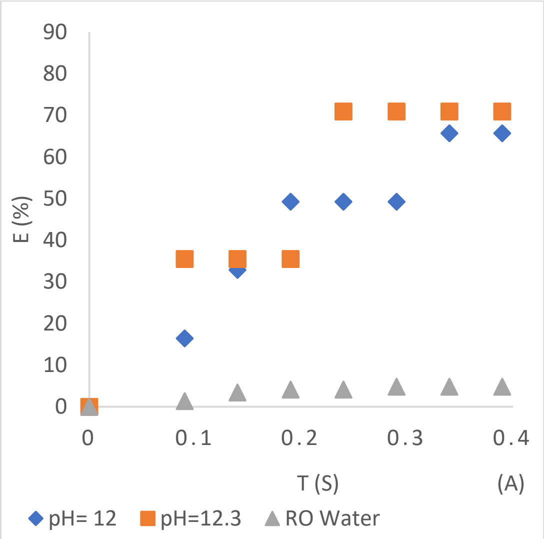

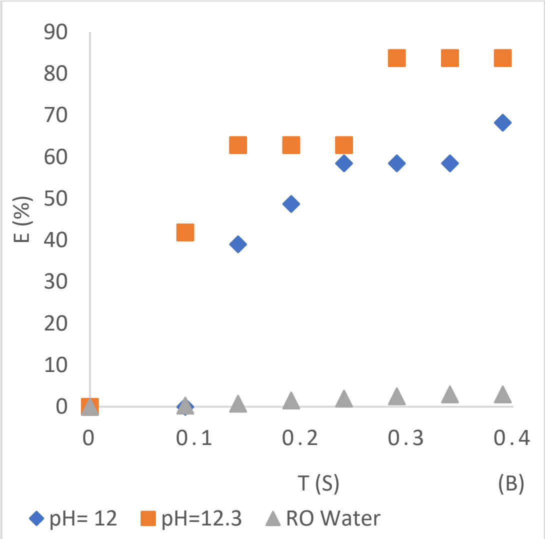

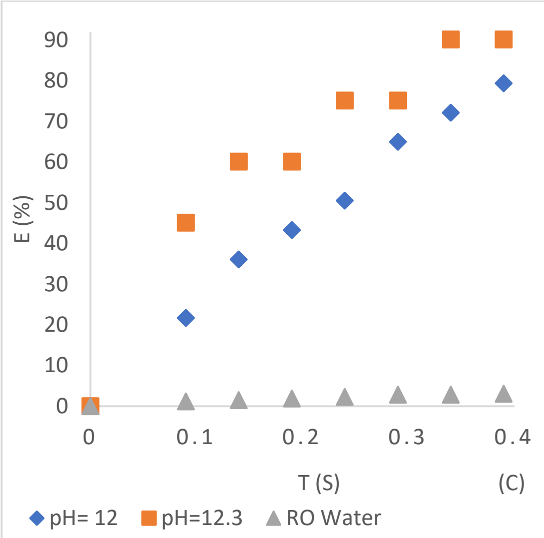

Figure 8 The effect of the concentration of NaOH (pH) on the removal efficiency E of CO_2 (%) as a function of residence time t_{res} (s) at Ut = 2 $m.s^{-1}$ and: (A) 15% v/v CO_2, (B) 23 % v/v CO_2 and (C) 30 % v/v CO_2

3. *Effect of the volume content of CO_2 in the gas stream*

The effect of the volume content of CO_2 in the gas phase on its removal efficiency at pH = 12 is displayed in Figure 9 and that of pH = 12.3 is displayed in Figure 10. As the CO_2 volume content in the gas phase increases, at a specific total superficial velocity and solvent concentration, the removal efficiency increases. The reason behind this observation can be attributed to the instant reaction of CO_2 with the NaOH after its physical absorption, thus encouraging the mass transfer/absorption of CO_2 from the gas phase into the liquid phase. In chemical absorption, the reaction between the CO_2 and chemical solvents increases the rate of absorption (Glasscock, 1991) due to the reaction in the liquid phase, which removes the equilibrium partial pressure therefore increasing the mass transfer, and the consumption of the CO_2 at the interface.

As for the effect of the concentration of CO_2 in the gas stream (% v/v CO_2) on the efficiency of removal of CO_2, Figure 9 and 10 will be used for this analysis. Figure 9 displays the variation of the removal efficiency of CO_2 (%), from a gas stream of 15%, 23% and 30% v/v CO_2, as a function of the residence time at the four studied total superficial velocities (Ut = 1, 1.3, 1.6, 2 $m.s^{-1}$) using a liquid stream of pH = 12 and of pH = 12.3 in Figure 10. The highest recorded removal efficiencies, when the concentration of NaOH and the total superficial velocity are kept constant, correspond to the highest concentration of CO_2 in the gas stream. In Figure 10 (D), the highest recorded efficiency of removal of 83.2% at pH = 12 was obtained at $U_t = 2$ $m.s^{-1}$ and 30 % v/v CO_2. Consider Figure 10 (A), at a pH=12.3 and $U_t = 1$ $m.s^{-1}$, when the % v/v CO_2 = 15%, the efficiency of removal kept on increasing until it reached a maximum of 54.22%, and remained constant all throughout the column. Increasing the % v/v CO_2 to 30%, the efficiency of removal of CO_2 kept increasing until it reached a maximum of 57.4% at a height of 68 cm after 0.68 s. These observations allow

Therefore, an increase in the total superficial velocity or the volume content of CO_2 in the gas phase or the concentration of the solvent directly leads to an increase in the removal efficiency of CO_2. Increasing the total superficial velocity or the concentration of the solvent (pH) would enable the possibility of reducing the length of the reactor.

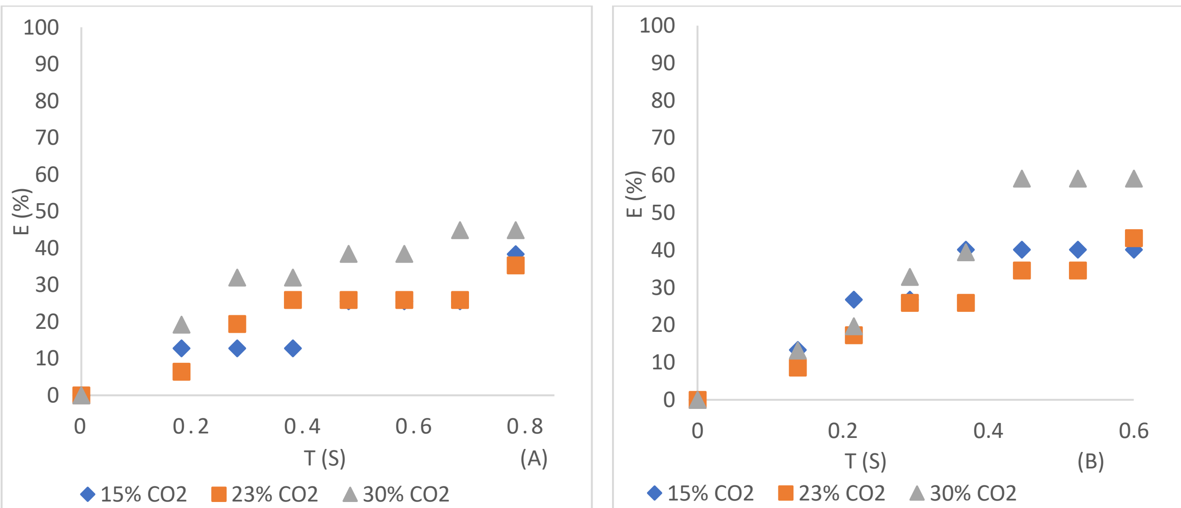

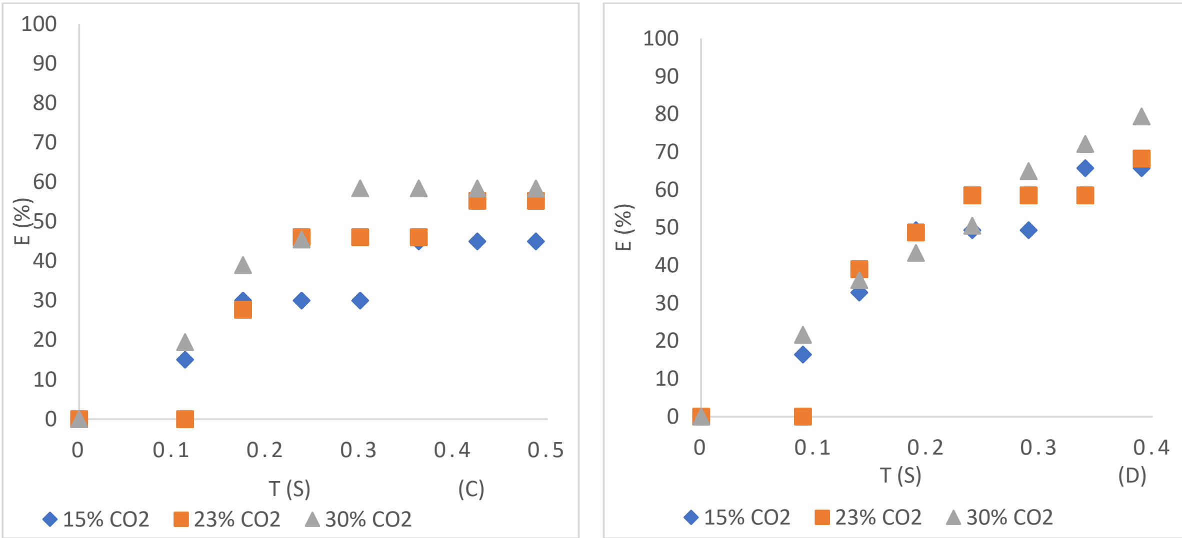

Figure 9 The effect of the volume content of CO_2 in the gas phase (% v/v CO_2) on the removal efficiency E of CO_2 (%) as a function of residence time t_{res} (s) at total superficial velocities Ut: (A) 1 $m.s^{-1}$, (B) 1.3 $m.s^{-1}$, (C) 1.6 $m.s^{-1}$ and (D) 2 $m.s^{-1}$ at pH=12.

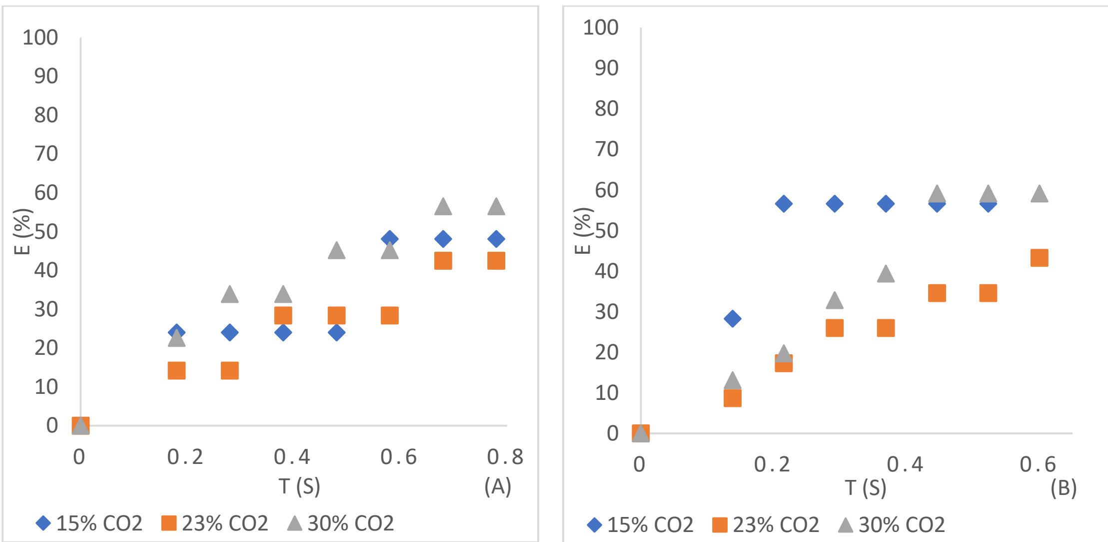

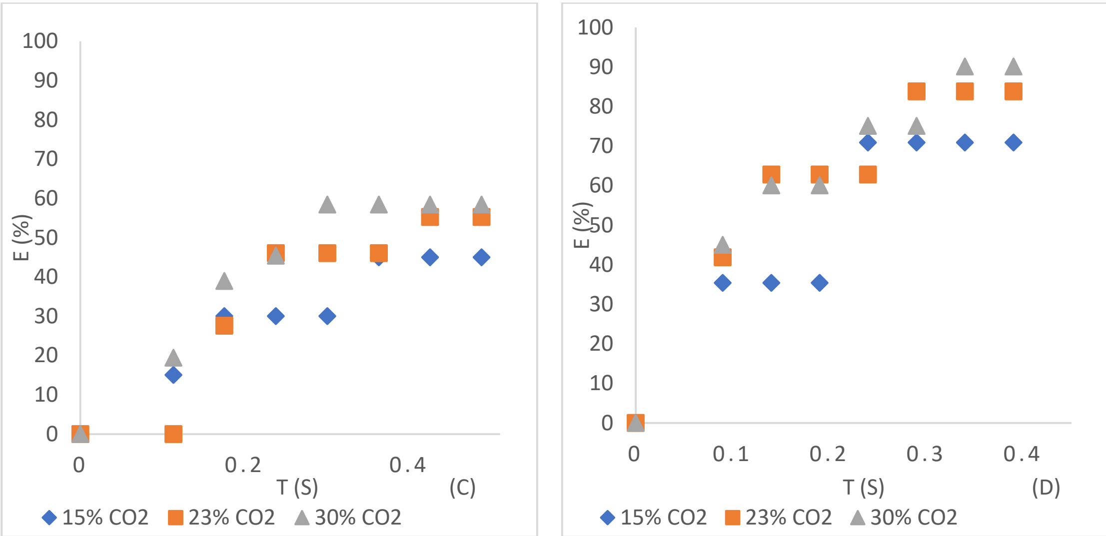

Figure 10 The effect of the volume content of CO_2 in the gas stream (% v/v CO_2) on the removal efficiency E of CO_2 (%) as a function of residence time t_{res} (s) at total superficial velocities Ut: (A) 1 m.s^{-1}, (B) 1.3 m.s^{-1}, (C) 1.6 m.s^{-1} and (D) 2 m.s^{-1} at pH=12.3.

B. Energy requirements

Computing the energy requirement to remove CO_2 is a factor that needs to be considered when assessing the economic feasibility of a process. E_{CO2}, the energy needed to absorb a unit mass of CO_2, will only be presented since it takes into consideration the mass of CO_2 absorbed by the solvent.

According to Equation 9, the main parameters that affect the energy consumption per unit mass of CO_2 , E_{CO2}, are the pressure drop, the CO_2 concentration difference between the inlet and the outlet of the reactor and the total superficial velocity. Therefore, as the pressure drop or total superficial velocity increases, the energy consumption rate increases. According to Figure 11, as the total superficial velocity increases the pressure drop directly increases, which confirms the previous observation. When comparing the pressure drop values at either pH = 12 or 12.3, under the same operational conditions mentioned in Figure 11, we can notice that the pressure drop is almost identical, thus proving that the slight difference of concentration of NaOH in the liquid phase doesn't significantly affect the pressure drop in the column, whereas for the runs using RO water as the solvent the pressure drop was higher, which indicates that incorporating a chemical reaction in the carbon capture process reduces the pressure drop in the column.

According to Equation 9, as the amount of absorbed CO_2 between the inlet and the outlet of the reactor increases, E_{CO2} decreases. Therefore, the higher the removal efficiency of CO_2, which indicates that a higher concentration of CO_2 was absorbed, the E_{CO2} becomes lower. In Figure 12, as the total superficial velocity increased, the CO_2 concentration gradient increased due to the increase in generated turbulence, which causes an increase in interfacial area of contact between the gas and liquid phases, through bubble breakage and dispersion, thus increasing the mass transfer and the concentration of CO_2 absorbed by the solvent. As the concentration of the solvent increases, the removal efficiency, at the same total superficial velocity, increases due to the increase in absorption capacity and higher OH^- concentration to react with the dissolved CO_2, thus absorbing CO_2 at a faster rate and increasing the CO_2 concentration gradient. Finally, as the CO_2 volume content of the gas stream increases, the absorption rate increases due to the increase in concentration gradient at the interface, which increases the concentration gradient of CO_2 absorbed by the solvent between the inlet and the outlet of the reactor.

Figure 13 displays the variation of the CO_2 removal efficiency as a function of E_{CO2} at a pH=12 and 12.3. As the power consumption, E_{CO2}, into the reactor increases, the CO_2 removal efficiency E will increase as well due to the increased induced turbulence caused by the higher total superficial velocity. When using a gas stream of any CO_2 volume content, higher CO_2 removal efficiencies were recorded at a lower energy consumption rate, when the solvent has a higher concentration. The highest E_{CO2} value recorded in this study was of 377 KW.h/tonne-CO_2 was obtained at U_T = 1.6 m/s and pH= 12 and % v/v CO_2 = 15%. This verifies that as the CO_2 volume content of the gas stream and the concentration of the solvent increases, the energy consumption rate at the same superficial velocity decreases. At the same CO_2 volume content of the gas stream and using the same solvent concentration, as the total superficial velocity increases the power consumption rate to absorb a unit mass of CO_2 increases.

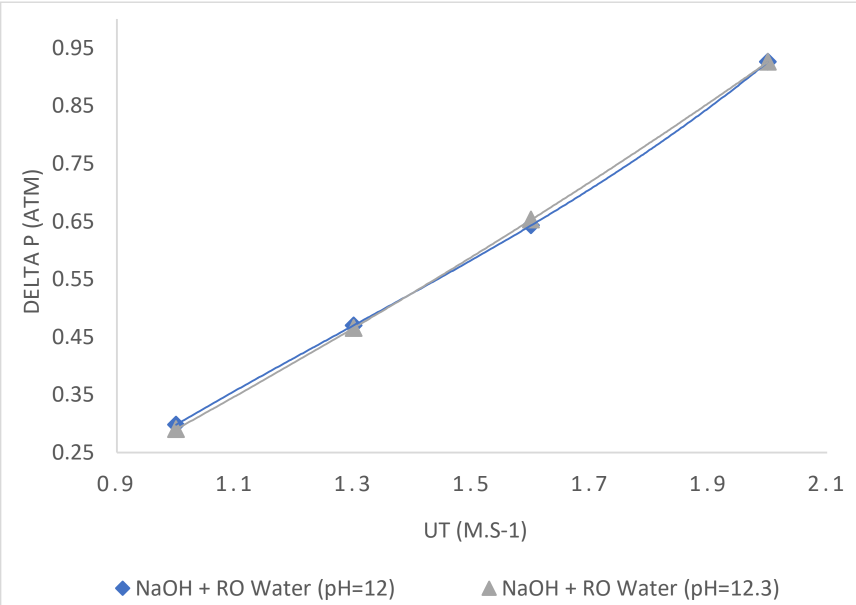

Figure 11 The variation of the ΔP (atm) as a function of the total superficial velocity Ut (m.s-1) using a gas stream of 15% CO_2 and a liquid stream containing NaOH and RO water mixture (pH=12 and 12.3) and pure RO water.

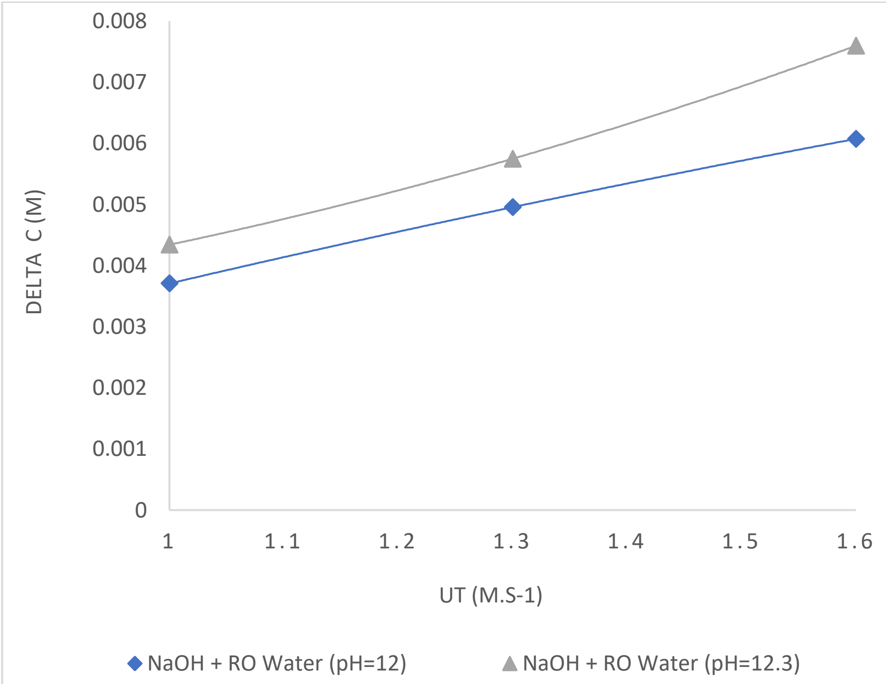

Figure 12 The variation of the ΔC of CO_2 (M) as a function of the total superficial velocity Ut (m.s-1) using a gas stream of 15% CO_2 and a liquid stream containing NaOH and RO water mixture (pH=12 and 12.3) and pure RO water.

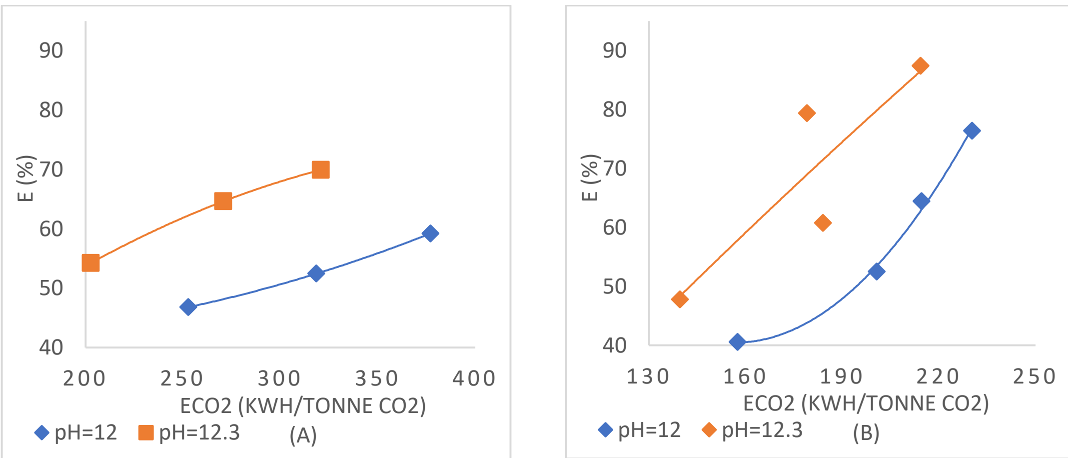

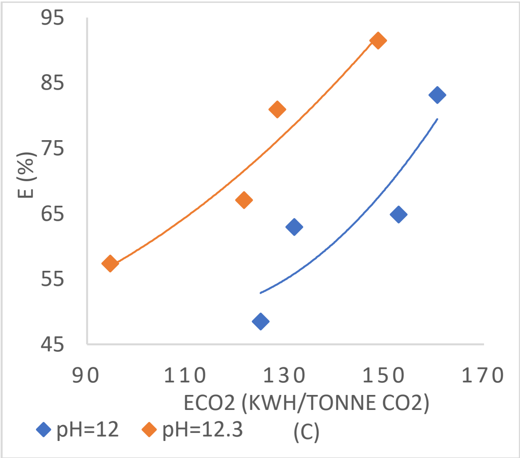

Figure 13 CO_2 removal efficiency E (%) versus the energy needed to process a mass unit of absorbed CO_2, E_{CO2}, at different pH values: (A) % v/v CO_2 = 15%, (B) % v/v CO_2 = 23% and (C) % v/v CO_2 = 30%.

CHAPTER V
CONCLUSIONS AND RECOMMENDATIONS

Carbon capture intensification was investigated in a tubular reactor equipped with screen-type static mixers at different experimental conditions. In this reactor, the effects of the total superficial velocity, the concentration of the solvent and the volume content of CO_2 in the gas stream on the chemical absorption of CO_2 were investigated.

In order to be able to properly assess the effects of the previously mentioned parameters, the following elements were evaluated: CO_2 removal efficiency and energy consumption per unit mass of absorbed CO_2. It was found that removal efficiency of CO_2 increased with an increase in the total superficial velocity, CO_2 volume content in the gas phase and solvent concentration (pH). The removal efficiency reached elevated values of 91.45% (U_T = 2 m/s, %v/v CO_2 = 30% and pH = 12.3) at an energy requirement of 148.65 kW.h/tonne-CO_2 absorbed. Also, increasing the total superficial velocity or the concentration of the solvent (pH) would allow the possibility of reducing the length of the reactor.

Based on the results obtained, it is possible to conclude that:

- The removal efficiencies of CO_2 using NaOH aqueous solution as the solvent were 16 to 30 times greater than those using RO water as the solvent, further highlighting the superiority of chemical absorption over physical absorption in carbon capture.
- Operating at high total superficial velocity, high CO_2 concentration and high NaOH concentration intensified chemical absorption of CO_2 into the solvent and equilibrium was reached at lower residence times.

- By tracking the removal efficiency, minimizing the height of the reactor can be achieved, thereby reducing the energy requirement and maintenance costs.
- By tracking the concentration of OH^- entering and exiting the reactor, recycling the solvent leaving the system can be realized thus reducing operating costs (less solvent used, less waste generated and lower energy requirement).
- The energy consumption rate to absorb a unit mass of CO_2 decreases as the removal efficiency increases (higher concentration of solvent or higher CO_2 volume content in the gas stream) and increases as the total superficial velocity increases (higher pressure drop due to a rise in friction between the particles and the walls of the reactor).

APPENDIX I

RAW EXPERIMENTAL DATA

In the results below, P represents the volume of the titrant that was added to the prepared sample to reach the first equivalence point and T represents the volume of the titrant in mL that was added to reach the second equivalence point, according to the standard titration method. P_{in} and P_{out} represent the pressures at the inlet and outlet of the reactor in bar, and U_T is the total superficial velocity in m/s.

1. *Mn* = 80, φ = 20%, %CO_2 =15%, pH=12

U_T	1		1.3		1.6		2	
P_{in}	1.32122449		1.520272109		1.72122449		2.012857143	
P_{out}	1.023197279		1.050190476		1.078061224		1.086870748	
Sample	P	T	P	T	P	T	P	T
0	9	10.5	8.5	10.1	8.2	9.9	7.1	8.6
1	9	10.6	8.2	9.9	8.2	10	7.3	8.9
2	8.8	10.4	8.4	10.2	8	9.9	7.1	8.8
3	9	10.6	8.2	10	7.9	9.8	6.5	8.3
4	8.8	10.5	8.3	10.2	8	9.9	6.7	8.5
5	9	10.7	8.1	10	8.1	10.1	6.5	8.3
6	9.2	10.9	8	9.9	7.9	9.9	6.6	8.5
7	8.9	10.7	8.4	10.3	8	10	6.5	8.4

2. Mn = 80, φ = 20%, %CO_2 =23%, pH=12

U_T	1		1.3		1.6		2	
P_{in}	1.334829932		1.496462585		1.714829932		1.977619048	
P_{out}	1.027346939		1.045646259		1.068693878		1.074659864	
Sample	P	T	P	T	P	T	P	T
0	9.5	11	8	10.2	8	9.6	9.2	11
1	8.8	10.4	8.3	10.6	8.2	9.8	9	10.8
2	8.7	10.5	8.4	10.8	7.8	9.7	8.5	10.7
3	8.8	10.7	7.8	10.3	7.7	9.8	8.2	10.5
4	8.7	10.6	8	10.5	7.6	9.7	8.1	10.5
5	8.8	10.7	8.2	10.8	7.6	9.7	8	10.4
6	9.2	11.1	7.9	10.5	7.8	10	8.1	10.5
7	9.1	11.1	8.2	10.9	7.6	9.8	8	10.5

3. Mn = 80, φ = 20%, %CO_2 =30%, pH=12

U_T	1		1.3		1.6		2	
P_{in}	1.335782313		1.532040816		1.731292517		2.015034014	
P_{out}	1.027346939		1.055170068		1.075170068		1.076190476	
Sample	P	T	P	T	P	T	P	T
0	9.3	10.9	8.9	10.7	8.5	10.1	8.9	10.9
1	8.7	10.6	8.6	10.6	8.3	10.2	8.9	11.2

2	8.6	10.7	8.5	10.6	7.4	9.6	8.1	10.6
3	8.3	10.4	8.4	10.7	7.5	9.8	7.9	10.5
4	8.4	10.6	8.3	10.7	7.4	9.9	7.8	10.5
5	8.7	10.9	7.9	10.6	7.7	10.2	7.6	10.5
6	8.4	10.7	8.1	10.8	7.3	9.7	7.4	10.4
7	8.6	10.9	7.9	10.6	7.3	9.8	7.3	10.4

4. *Mn* = 80, φ = 20%, %CO_2 =15%, pH=12.3

U_T	1		1.3		1.6		2	
P_{in}	1.314489796		1.519931973		1.735510204		2.012857143	
P_{out}	1.024217687		1.054353741		1.082653061		1.086870748	
Sample	P	T	P	T	P	T	P	T
0	8.3	9.7	7.2	8.2	6.9	7.9	10.7	11.9
1	8.7	10.2	7.1	8.2	6.7	7.8	9.7	11
2	8.5	10	6.9	8.1	6.2	7.3	9.8	11.1
3	8.6	10.1	7.1	8.3	6.4	7.5	9.5	10.8
4	8.4	9.9	7.2	8.4	6.5	7.7	9.7	11.1
5	8.6	10.2	7.4	8.6	6.5	7.7	9.5	10.9
6	8.3	9.9	7.2	8.4	6.4	7.6	9.4	10.8
7	8.2	9.8	7.1	8.3	6.4	7.6	9.8	11.2

5. *Mn* = 80, φ = 20%, %CO_2 =23%, pH=12.3

U_T	1	1.3	1.6	2

P_{in}	1.319659864		1.514013605		1.741836735		2.011156463	
P_{out}	1.023197279		1.048367347		1.079863946		1.088571429	
Sample	P	T	P	T	P	T	P	T
0	9.2	11	7.8	9.4	8.7	9.9	9.4	10.8
1	9.6	11.5	7.9	9.6	8.5	9.8	9.5	11.1
2	9.5	11.4	7.9	9.7	8.3	9.7	9.2	10.9
3	9.3	11.3	7.9	9.7	8.2	9.7	9.1	10.8
4	9.4	11.4	7.7	9.6	8.4	9.9	9.2	10.9
5	9.3	11.3	7.8	9.7	8.2	9.7	9	10.8
6	9.5	11.6	7.7	9.6	8	9.6	9.1	10.9
7	9.2	11.3	7.8	9.7	8.4	10	9	10.8

6. *Mn* = 80, φ = 20%, %CO_2 =30%, pH=12.3

U_T	1		1.3		1.6		2	
P_{in}	1.337006803		1.539659864		1.759931973		2.015034014	
P_{out}	1.029387755		1.061020408		1.082993197		1.087755102	
Sample	P	T	P	T	P	T	P	T
0	10.4	11.9	8.3	9.8	7.5	8.5	9.2	10.7
1	10	11.7	8.3	9.9	7.2	8.5	9.2	11
2	9.9	11.7	8.4	10.2	7	8.5	9	10.9
3	9.9	11.7	8.3	10.2	7.1	8.6	9	10.9
4	9.8	11.7	8.2	10.1	7	8.5	9	11
5	9.9	11.8	8.2	10.2	6.9	8.5	8.8	10.8

6	9.7	11.7	8.3	10.3	7.1	8.7	8.6	10.7
7	10	12	8.2	10.2	7	8.6	8.9	11

7. *Mn* = 80, φ = 20%, %CO_2 =15% (RO water used as a solvent)

U_T	1		1.3		1.6		2	
P_{in}	1.423809524		1.596734694		1.838095238		2.089251701	
P_{out}	1.04707483		1.063870748		1.072244898		1.105442177	
Sample	P	T	P	T	P	T	P	T
0	87.5	90	92	96	93.7	97.7	92.7	96.7
1	93.5	96	91.7	95.9	96.6	101	98.6	102.8
2	93.5	96.2	92.1	96.5	94.1	98.5	96.1	100.6
3	92.8	95.6	92	96.5	91.9	96.4	93	97.6
4	93.1	96	92.6	97.1	94	98.5	94.2	98.8
5	92.4	95.3	91.5	96	92	96.6	92.1	96.8
6	92.8	95.7	92.4	97	92.3	96.9	93.2	97.9
7	92.5	95.4	91.4	96	92	96.7	91.9	96.7

8. *Mn* = 80, φ = 20%, %CO_2 =23% (RO water used as a solvent)

U_T	1		1.3		1.6		2	
P_{in}	1.438095238		1.606190476		1.82952381		2.093061224	
P_{out}	1.046802721		1.062040816		1.077823129		1.105238095	
Sample	P	T	P	T	P	T	P	T
0	93.2	97	93	97	91.1	96	91	96

1	93.4	97.3	93	97.3	91	96.1	91.3	96.4
2	94.5	98.6	94.2	98.7	91.2	96.6	91.2	96.5
3	96	100.4	95.1	99.8	91.4	96.9	91.1	96.7
4	92.8	97.6	91.8	96.5	91.1	96.7	90.6	96.4
5	91.4	96.3	91.2	96.2	91.3	97.1	90.6	96.6
6	92.7	97.7	92.3	97.3	91.4	97.2	91.3	97.5
7	92.1	97.1	91.5	96.6	91.3	97.3	91.1	97.3

9. *Mn* = 80, φ = 20%, %CO_2 =30% (RO water used as a solvent)

U_T	1		1.3		1.6		2	
P_{in}	1.442857143		1.606802721		1.822244898		2.122721088	
P_{out}	1.047414966		1.067346939		1.081088435		1.112244898	
Sample	P	T	P	T	P	T	P	T
0	91.1	94.7	92.5	96.3	92.7	96.6	92.4	96.4
1	91	95	90.8	95.1	90.6	95.1	91.2	95.8
2	91.2	95.5	91	95.7	91.1	95.7	91.4	96.2
3	91.4	95.9	91.1	95.9	91.3	96.3	91.6	96.6
4	91.1	95.8	91.2	96.2	91	96.4	91.8	97
5	91.3	96.1	91	96.2	91.1	96.6	92.2	97.7
6	91.4	96.5	91.2	96.6	91.2	96.8	92	97.5
7	91.3	96.5	91	96.4	91.3	96.9	92.1	97.7

APPENDIX II

SAMPLE CALCULATION

A sample calculation for computing k_La is provided in this section for two chosen experimental runs. The first run used an aqueous solution of NaOH and RO water as the solvent and a pH=12, having the conditions mentioned in Table 5.

Table 5: Experimental Conditions of the First Experimental Run

Condition	**Value**
Mesh Number	80
Number of screen elements	15
Inter screen spacing (mm)	40
Screen open area (%)	31.36
Dispersed phase holdup (%)	25.52
Water flow rate, Q_L, (L/min)	23.9
Gas flow rate, Q_g, (L/min)	6.1
CO_2 flow rate, Q_g (L/min)	0.9
Air flow rate, Q_g (L/min)	5.2
Temperature (K)	295

As previously mentioned k_La is obtained from plotting $\ln\left(C^*_{CO_2} - C\right)$ versus t. Therefore, t, $C^*_{CO_2}$ and C should be calculated first.

The residence time is calculated using the total superficial velocity,

$$t = \frac{d}{U_T} \qquad [12]$$

Where U_T is determined from the gas and liquid flow rates as shown below:

$$U_T\ (m/s) = \frac{Q_L + Q_g}{1000 \times 60 \times Ac} = 0.989 \qquad [13]$$

and Ac is the cross-section area of the column and is equal to:

$$Ac = \frac{\pi D^2}{4} = \frac{\pi(0.025^2)}{4} = 4.90625 \times 10^{-4}\ m^2 \qquad [14]$$

C, the concentration of CO_2 in the liquid phase in the form of CO_3^{2-}, is calculated according to Warder and Winkler's method. For example, at sample 2

$$C\ \left(\frac{mol}{L}\right) = \frac{(T-P).C_{acid}}{v\ sample} \qquad [15]$$

P (mL)	T (mL)	Acid Concentration (M)	C (M)
8.8	10.4	0.01	0.0032

To calculate $C^*_{CO_2}$, knowledge of the local partial pressure of CO_2 is needed and obtained by assuming that $\frac{\Delta P}{\text{Length of the reactor}}$ is constant for each experiment. Therefore, the local pressure at each sampling point is calculated from the following equation:

$$P_x = P_{bottom} - \frac{\Delta P}{\text{Length of the reactor}}.X \qquad [16]$$

Where X = length from the pressure sensor at the bottom of the reactor to the sampling point;

For example, $\frac{\Delta P}{\text{Length of the reactor}}$ = 0.003137129 atm/cm and P_{bottom} = 1.32122449 atm. At sampling point 2 (x = 28 cm), $P_{x\,=\,28\ cm}$ = 1.233384891 atm.

Then, the local partial pressure of CO_2 at this point is

$$P_{CO_2} = P_x . y \quad [17]$$

Where y = local mole fraction of CO_2

The last step in determining $C^*_{CO_2}$ is to calculate it from Henry's law which is calculated according to equation [9-12] found in the methodology section.

Henry's law of CO_2 in water is calculated according to equation 10 and is 0.032552006 kmol/(m^3.bar). Then, henry's constant in an electrolyte solution is calculates using equation [9-12] according to the values found in

Table 3.

Table 3 Ionic strength calculation

Ions	Concentration of Ions (M)	Ionic Strength
Na^+	0.13373	0.13373
K^+	0.0000375	0.0000375
OH^-	0.008456646	-0.008456646
CO_3^{2-}	0.004688833	-0.009377667

Therefore, the Henry's constant of CO_2 in an electrolyte solution turns out to be 0.03150141 kmol/(m^3.bar).

APPENDIX III

ERROR ANALYSIS

In this investigation, the physical quantities directly measured are subject to errors associated with the instruments used.

Table 4 presents the errors associated with each measured physical quantity.

Table 4 Errors associated with the physical quantities

Physical quantity measured	Error
Q_L	5%
Q_g	4%
Volume in burette	0.05 mL
Pressure transducer	0.4 kPa

To calculate the propagated error on the evaluation parameter, the following equation was used.

$$\Delta y_i = y(x_1, x_2, \dots, x_i + \Delta x_i, \dots, x_n) - y(x_1, x_2, \dots, x_n) \qquad [18]$$

1. Error on $\frac{\Delta P}{screen}(kPa)$:

$$Error\ on\ \frac{\Delta P}{screen}(kPa) = \frac{\Delta P_{bottom} - \Delta P_{top}}{15} = \frac{0.4 + 0.4}{15} = 0.05333 \qquad [19]$$

2. Error on U_T (m/s):

The error on U_T is given by the following equation

$$\Delta U_T\ (m/s) = \Delta U_L + \Delta U_g \qquad [20]$$

Sample calculation displayed in Table 5:

Table 5 Sample calculation of the error on U_T = 2 m/s

U_{gas} (m/s)	ΔU_{gas} (m/s)	U_L (m/s)	ΔU_L (m/s)	ΔU_T (m/s)
0.3	0.012	1.62	0.081	0.093

3. Error on time

From ΔU_T the error on residence time (Δt) can be calculated as shown below:

$$\Delta t\ (s) = t - \frac{d}{U_T + \Delta U_T} \quad [21]$$

$$\%\ error\ (\Delta t) = \frac{\Delta t}{t} \times 100 \quad [22]$$

Table 6 Calculation of the error on t for the condition % v/v CO_2 = 30% and U_t = 2 $m.s^{-1}$

U_T (m/s)	ΔU_T (m/s)	t (s)	Δt (s)	Δt (%)
2	0.093	0.39	0.0175	4.487

4. Error on $[CO_3^{2-}]$

The error on the $[CO_3^{2-}]$ propagates from the volume read from the burette. Therefore,

$$[CO_3^{2-}]_{(e)} = \frac{C_a.(T - P + \Delta V)}{V_{sample}} \quad [23]$$

Where, $[CO_3^{2-}]_{(e)}$ = concentration of CO_3^{2-} including the error in reading the burette; M

ΔV = error in reading the volume from the burette; mL

C_a = concentration of the acid; M

V_{sample} = volume of the sample; mL

The error would be then:

$$\% \, error \, [CO_3^{2-}] = \frac{[CO_3^{2-}]_{(e)} - [CO_3^{2-}]}{[CO_3^{2-}]} x \, 100 \qquad [24]$$

Table 7 Estimation of the % error on Efficiency for the condition U_t = 2 m/s and %v/v CO_2 = 30% at pH= 12 and 12.3

U_L (m/s)	ΔU_L (m/s)	$[CO_3^{2-}]$ (M)	$[CO_3^{2-}]_{(e)}$(M)	Efficiency (%)	Efficiency with the error (%)	% Error in Efficiency (%)
1.62	1.701	0.0062	0.0069	73.39	75	2.2
1.62	1.701	0.0084	0.0088	90.15	92.3	2.38

5. Error on E_{CO2}

The E_{CO2} for the specified experimental run is 160.6218588 kWh/tonne of CO_2 at pH = 12 and 148.6466271 kWh/tonne CO_2 at pH = 12.3

The error on E_{CO2} was calculated by determining ΔE_{spm} as shown below:

$$\Delta E_{CO_2} (kWh/tonne \;\; of \;\; CO_2) = E_{CO_2} - \frac{(\Delta P + 0.0533) \cdot (Q_L + \Delta Q_L + Q_G + \Delta Q_G)}{(Q_G + \Delta Q_G). M_{CO_2}. \Delta C_{CO_2}} \qquad [25]$$

The percentage error on E_{spm} is calculated as follows:

$$\% \, error \left(E_{CO_2}\right) = \frac{\Delta E_{CO_2}}{E_{CO_2}} \times 100 \qquad [26]$$

Therefor the ΔE_{CO_2} at pH= 12 is 0.3936 KW.h/tonne CO_2 and at pH = 12.3 is 0.4177 KW.h/tonne CO_2. Therefore, the $\% \, error \left(E_{CO_2}\right)$ = 0.246 % and 0.281% respectively.

REFERENCES

A. Aboudheir, P. Tontiwachwuthikul, A. Chakma, R. Idem, 2003, Kinetics of the reactive absorption of carbon dioxide in high CO_2-loaded, concentrated aqueous monoethanolamine solutions, Chem Eng Sci, 58, 5195-5210

Abanades JC, Arias B, Lyngfelt A, Mattisson T, Wiley DE, Li H, et al. Emerging CO_2 capture systems. Int. J. Greenh. Gas Contr. 2015;40:126–66

Abou Hweij, K., Azizi, F., 2015. Hydrodynamics and residence time distribution of liquid flow in tubular reactors equipped with screen-type static mixers. Chem. Eng. J. 279, 948–963.

Akbari M, Peyvand V-e-S (2019) CO_2 equilibrium solubility in and physical properties for monoethanolamine glycinate at low pressures. Process safety and environmental protection, vol 132. Institution of Chemical Engineers.

Al Taweel, A. M.; Azizi, F.; Sirijeerachai, G. Static Mixers: Effective Means for Intensifying Mass Transfer Limited Reactions. Chem. Eng. Process. 2013, 72, 51−62

Al Taweel, A. M.; Yan, J.; Azizi, F.; Odedra, D.; Gomaa, H. G. Using In-Line Static Mixers to Intensify Gas-Liquid Mass Transfer Processes. Chem. Eng. Sci. 2005, 60, 6378−6390.

Al Taweel, A.M., Li, C., Gomaa, H.G., Yuet, P., 2007. Intensifying mass transfer between immiscible liquids: Using screen-type static mixers. Chem. Eng. Res. Des. 85, 760–765.

Allendorf MD, Bauer CA, Bhakta RK, Houk RJT (2009) Luminescent metal-organic frameworks. Chem Soc Rev 38(5):1330–1352.

Aroonwilas, A., 2001. MASS-TRANSFER WITH CHEMICAL REACTION IN

Aroonwilas, A., Veawab, A., Tontiwachwuthikul, P., 1999. Behavior of the Mass-Transfer Coefficient of Structured Packings in CO2 Absorbers with Chemical Reactions. Ind. Eng. Chem. Res. 38, 2044–2050.

Azizi, F., Al Taweel, A.M., 2015. Mass Transfer in an Energy-Efficient High-Intensity Gas-Liquid Contactor. Ind. Eng. Chem. Res. 54, 11635–11652.

Azizi, F.; Abou Hweij, K. Liquid-Phase Axial Dispersion of Turbulent Gas-Liquid Co-Current Flow Through Screen-Type Static Mixers. AIChE J. 2017, 63, 1390−1403.

Azizi, F.; Al Taweel, A. M. Hydrodynamics of Liquid Flow through Screens and Screen-Type Static Mixers. Chem. Eng. Commun. 2011, 198, 726−742.

Azizi, F.; Al Taweel, A. M. Mass Transfer in an Energy-Efficient High-Intensity Gas−Liquid Contactor. Ind. Eng. Chem. Res. 2015, 54, 11635−11652.

Baxter L, Baxter A, Burt S (2011) Cryogenic CO2 capture as a cost-effective CO2 capture process cryogenic CO2 capture as a cost-effective CO2 capture process. Int J Hydrogen Energy 36(16):10355–10365

Borhani TN, Oko E, Wang M. Process modelling and analysis of intensified CO2 capture using monoethanolamine (MEA) in rotating packed bed absorber. J Clean Prod 2018;204:1124–42.

Borhani TN, Oko E, Wang M. Process modelling, validation and analysis of rotating packed bed stripper in the context of intensified CO2 capture with MEA. J Ind Eng Chem 2019;75:285–95.

Budzyński, P., Gwiazda, A., & Dziubiński, M. (2017). Intensification of mass transfer in a pulsed bubble column. *Chemical Engineering and Processing: Process Intensification, 112*, 18-30. doi:10.1016/j.cep.2016.12.004

Chavez, R.-H., Guadarrama, J.J. De, 2010. Comparison of structured packings in CO2 absorber with chemical reactions, *in: Chemical Engineering Transactions.* pp. 577–582.

Chen, B.H., Vallabh, R., 1970. Holdup and Mass transfer in Bubble Columns Containing Screen Cylinders. Ind. Eng. Chem. Process Des. Dev. 9, 121–126.

Chen, P.C., Huang, C.F., Chen, H.W., Yang, M.W., Tsao, C.M., 2014. Capture of CO2 from coal-fired power plant with NaOH solution in a continuous pilot-scale bubble-column scrubber. Energy Procedia 61, 1660–1664.

Chen, P.C., Liao, C., 2014. A Study on CO2 Absorption in Bubble Column Using DEEA/EEA Mixed Solvent. Int. J. Eng. Pract. Res. 3, 78–82.

Chiang, C.-Y., Lee, D.-W., Liu, H.-S., 2017. Carbon dioxide capture by sodium hydroxide-glycerol aqueous solution in a rotating packed bed. J. Taiwan Inst. Chem. Eng. 72, 29–36.

Devries, N.P., 2014. CO2 Absorption into Concentrated Carbonate solutions with promoters at elavated temperatures. Environ. Regul.

Duss, M., Meierhofer, H., Nutter, D.E., 2001. Effective interfacial area and liquid holdup of Nutter Rings at high liquid loads. Chem. Eng. Technol. 24, 716–723.

European Commission, in Commission Staff Working Document: Energy Storage—The Role of Electricity (2017)

European Parliament, in Directive 2009/28/EC of the European Parliament and of the Council of 23 April 2009 (2009)

Eurostat, in Greenhouse Gas Emissions by Sector (source: EEA) (code: tsdcc210).

Evren, V., Çağatay, T., Özdural, A.R., 1999. Carbon dioxide-air mixtures: Mass transfer in recycling packed-bed absorption columns operating under high liquid flow rates. Sep. Purif. Technol. 17, 89–96.

Ferreira, B.S., Fernandes, H.L., Reis, A., Mateus, M., 1998. Microporous hollow fibres for carbon dioxide absorption: Mass transfer model fitting and the supplying of carbon dioxide to microalgal cultures. J. Chem. Technol. Biotechnol. 71, 61–70.

Fleischer, C., Becker, S., Eigenberger, G., 1996. Detailed modeling of the chemisorption of CO2 into NaOH in a bubble column. Chem. Eng. Sci. 51, 1715–1724.

Gabrielsen, J., Svendsen, H.F., Michelsen, M.L., Stenby, E.H., Kontogeorgis, G.M., 2007. Experimental validation of a rate-based model for CO2capture using an AMP solution. Chem. Eng. Sci. 62, 2397–2413.

Gavini, S., 2017. Mass transfer and process control in randomly packed column a case study on CO2 absorption with NaOH A Thesis Presented to the Department of Chemical Engineering California State University , Long Beach In Partial Fulfillment of the Requirements for the D.

Ghanem, A., Lemenand, T., Valle, D. Della, Peerhossaini, H., 2014. Static mixers: Mechanisms, applications, and characterization methods–A review. Chem. Eng. Res. Des. 92, 205–228.

Giri A, Pant D (2019) Carbonic anhydrase modification for carbon management. Environ Sci Pollut Res 27:1294–1318

Glasscock DA. Modelling and experimental study of carbon dioxide absorption into aqueous alkanolamines. 1991.

Guo, Y., Niu, Z., Lin, W., 2011. Comparison of removal efficiencies of carbon dioxide between aqueous ammonia and NaOH solution in a fine spray column. Energy Procedia 4, 512–518.

Hill, G.A., 2006. Measurement of overall volumetric mass transfer coefficients for carbon dioxide in a well-mixed reactor using a pH probe. Ind. Eng. Chem. Res. 45, 5796–5800.

Hsu, S.-C., Lu, C., Su, F., Zeng, W., Chen, W., 2010.*Thermodynamics and regeneration studies of CO2 adsorption on multiwalled carbon nanotubes. Chem. Eng. Sci*. 65, 1354–1361.

Hu, G., Nicholas, N.J., Smith, K.H., Mumford, K.A., Kentish, S.E., Stevens, G.W., 2016. Carbon dioxide absorption into promoted potassium carbonate solutions: A review. Int. J. Greenh. Gas Control 53, 28–40.

Ilea, F., Dragan, S. and Cormos, A., 2020. Assessment of mass transfer intensification potential for a CO2 capture process using three-phase fluidized bed. *Chemical Engineering and Processing - Process Intensification*, 157, p.108115.

Intergovernmental Panel on Climate Change, in Climate change 2014—Synthesis Report (2014)

International Energy Agency IEA, in CO2 Emissions Statistics (2018)

International Energy Agency, in CO2 Emissions from Fuel Combustion (2015)

Isa, F., Zabiri, H., Ng, N.K.S., Shariff, A.M., 2018. Purification of CO2removal via promoted potassium carbonate: A review on modelling & simulation techniques. Int. J. Greenh. Gas Control 76, 236–265.

Jain, D., Kuipers, J.A.M., Deen, N.G., 2015. Numerical modeling of carbon dioxide chemisorption in sodium hydroxide solution in a micro-structured bubble column. Chem. Eng. Sci. 137, 685–696.

Jiang J, Zhao B, Zhuo Y, Wang S (2014) Experimental study of CO2 absorption in aqueous MEA and MDEA solutions enhanced by nanoparticles. Int J Greenhouse Gas Control 29(2014):135–41.

Jie G, Yin J, Zhu F, Chen X, Tong M, Wanzhong K, Yartbo Z, Jun Lu (2016) Integrated study of a hybrid solvent MEA-methanol for post combustion carbon dioxide capture in packed bed absorption and regeneration. Sep Purif Technol 167(2016):17–23

Kaady, L.A., Azizi, F., Al-Hindi, M. Intensifying carbon capture using a small, flexible, and low-cost reactor; 2018.

Kamyab H, Chelliapan S, Lee CT, Khademi T, Nadda A, Yadav KK et al (2019a) Improved production of lipid contents by cultivating Chlorella pyrenoidosa in heterogeneous organic substrates. Clean Technol Environ Policy.

Keblinski P, Eastman JA, Cahill DG (2005) Nanofluids for thermal transport. Mater Today 8(6):36– 44.

Keshishian N, Nasr Esfahany M, Etesami N (2013) Experimental investigation of mass transfer of active ions in silica nanofluids. Int Commun Heat Mass Transfer 46(2013):148–53.

Kidnay AJ, Parrish WR. Fundamentals of natural gas processing. CRC Press; 2006.

Kim JH, Jung CW, Kang YT (2014) Mass transfer enhancement during CO2 absorption process in methanol/Al2O3 nanofluids. Int J Heat Mass Transfer 76(2014):484–91.

Kim JK, Jung JY, Kang YT (2006) the effect of nano-particles on the bubble absorption performance in a binary nanofluid. Int J Refrig 29(1):22–29.

Kim, D.M., Cho, J., 2011. A comparative study of carbon dioxide capture capabilities between methanol solvent and aqueous monoethanol amine solution. Korean J. Chem. Eng. 28, 22–26.

Kim, Y.E., Lim, J.A., Jeong, S.K., Yoon, Y. Il, Bae, S.T., Nam, S.C., 2013. Comparison of carbon dioxide absorption in aqueous MEA, DEA, TEA, and AMP solutions. Bull. Korean Chem. Soc. 34, 783–787.

Kim, Y.-S., Yang, S.-M., 2000. Absorption of carbon dioxide through hollow fiber membranes using various aqueous absorbents. *Sep. Purif. Technol. 21*, 101–109.

Koglin, B., Pawlowski, J., Schn??ring, H., 1981. Kontinuierliches Emulgieren mit Rotor/Stator???Maschinen: Einflu?? der volumenbezogenen Dispergierleistung und der Verweilzeit auf die Emulsionsfeinheit. Chemie Ing. Tech. 53, 641–647.

Kordylewski, W., Sawicka, D., Falkowski, T., 2013. Laboratory tests on the efficiency of carbon dioxide capture from gases in NaOH solutions. J. Ecol. Eng. 14, 54–62.

Koronaki IP, Prentza L, Papaefthimiou V. Modeling of CO2 capture via chemical absorption processes − an extensive literature review. Renew Sustain Energy Rev 2015;50:547–66.

Koronaki, I.P., Prentza, L., Papaefthimiou, V.D., 2017. Parametric analysis using AMP and MEA as aqueous solvents for CO 2 absorption 110, 126–135.

Kothandaraman, A., Nord, L., Bolland, O., Herzog, H.J., McRae, G.J., 2009. Comparison of solvents for post-combustion capture of CO2 by chemical absorption. Energy Procedia 1, 1373–1380.

Krauβ, M., Rzehak, R., 2017. Reactive absorption of CO_2 in NaOH: Detailed study of enhancement factor models. Chem. Eng. Sci. 166, 193–209.

Kumar, S., Cho, J.H., Moon, I., 2014. Ionic liquid-amine blends and CO2BOLs: Prospective solvents for natural gas sweetening and CO2capture technology-A review. Int. J. Greenh. Gas Control 20, 87–116.

Lee J, Farha OK, Roberts J, Scheidt KA, Nguyen ST, Hupp JT (2009) Metal-organic framework materials as catalysts. Chem Soc Rev 38(5):1450–1459.

Leung DYC, Caramanna G, Maroto-Valer MM. An overview of current status of carbon dioxide capture and storage technologies. Renew Sustain Energy Rev 2014;39:426–43.

Li JR, Ma Y, McCarthy MC, Sculley J, Yu J, Jeong HK, Balbuena PB, Zhou HC (2011) Carbon dioxide capture-related gas adsorption and separation in metal-organic frameworks. Coord Chem Rev 255(15–16):1791–1823.

Li T, Keener TC. A review: desorption of CO2 from rich solutions in chemical absorption processes. Int. J. Greenh. Gas Contr. 2016;51:290–304.

Lin, C.C., Kuo, Y.W., 2016. Mass transfer performance of rotating packed beds with blade packings in absorption of CO2 into MEA solution. Int. J. Heat Mass Transf. 97, 712–718.

Lin, C.-C., Liu, W.-T., Tan, C.-S., 2003. Removal of Carbon Dioxide by Absorption in a Rotating Packed Bed. Ind. Eng. Chem. Res. 42, 2381–2386.

Lisitsin, D., Hasson, D., Semiat, R., 2008. The potential of CO2 stripping for pretreating brackish and wastewater desalination feeds. Desalination 222, 50–58.

Luo, Y., Chu, G.W., Zou, H.K., Zhao, Z.Q., Dudukovic, M.P., Chen, J.F., 2012b. Gas-liquid effective interfacial area in a rotating packed bed. Ind. Eng. Chem. Res. 51, 16320–16325.

Luo, Y., Luo, J.Z., Chu, G.W., Zhao, Z.Q., Arowo, M., Chen, J.F., 2017. Investigation of effective interfacial area in a rotating packed bed with structured stainless steel wire mesh packing. Chem. Eng. Sci. 170, 347–354.

M. Wang, S.J. Atuman, C. Ramshaw, D. Eimer, N.M. Musa, Process intensification for post-combustion CO2 capture with chemical absorption: a critical review, Appl. Energy 158 (2015) 275–291.

MacDowell, N., Florin, N., Buchard, A., Hallett, J., Galindo, A., Jackson, G., Adjiman, C.S., Williams, C.K., Shah, N., Fennell, P., 2010. An overview of CO2capture technologies. Energy Environ. Sci. 3, 1645–1669.

Mahmoudkhani, M., Keith, D., 2009. Low-energy sodium hydroxide recovery for CO2 capture from atmospheric air—Thermodynamic analysis. International Journal of Greenhouse Gas Control, 3, 376-384

Mandal, B.P., Guha, M., Biswas, A.K., Bandyopadhyay, S.S., 2001. Removal of carbon dioxide by absorption in mixed amines: Modelling of absorption in aqueous MDEA/MEA and AMP/MEA solutions. Chem. Eng. Sci. 56, 6217–6224.

Mumford KA, Wu Y, Smith KH, Stevens GW. Review of solvent based carbon-dioxide capture technologies. Front Chem Sci Eng 2015;9:125–41.

N.borhani, T., & Wang, M. (2019). Role of solvents in CO2 capture processes: The review of selection and design methods. *Renewable and Sustainable Energy Reviews, 114*, 109299. doi: 10.1016/j.rser.2019.109299

NASA Goddard Institute for Space Studies, in GISS Surface Temperature Analysis (GISTEMP) (2017)

Nieves-Remacha, M.J., Kulkarni, A.A., Jensen, K.F., 2013. Gas–Liquid Flow and Mass Transfer in an Advanced-Flow Reactor. Ind. Eng. Chem. Res. 52, 8996–9010.

Niu, Z., Guo, Y., Lin, W., 2009. Experimental studies on CO2 capture in a spray scrubber using NaOH solution. 2009 Int. Conf. Energy Environ. Technol. ICEET 2009 3, 52–55.

Olajire, A.A., 2010. CO2 capture and separation technologies for end-of-pipe applications - A review. Energy 35, 2610–2628.

Olle B, Bucak S, Holmes TC, Lev Bromberg T, Hatton A, Wang DIC (2006) Enhancement of oxygen mass transfer using functionalized magnetic nanoparticles. Ind Eng Chem Res 45(12):4355–4363.

Pangarkar, V. G. (2017). Process intensification in multiphase reactors: From concept to reality. *Chemical Engineering and Processing: Process Intensification*, *120*, 1-8. doi:10.1016/j.cep.2017.06.004

Panja, N.C., Rao, D.P., 1993. Measurement of gas-liquid parameters in a mechanically agitated contactor. Chem. Eng. J. 52, 121–129.

Pei, S. L., Pan, S. Y., Li, Y. M., & Chiang, P. C. (2017). Environmental Benefit Assessment for the Carbonation Process of Petroleum Coke Fly Ash in a Rotating Packed Bed. Environmental Science & Technology, 51(18), 10674–10681. https://doi.org/10.1021/acs.est.7b00708.

Phan, D.T., Maeder, M., Burns, R.C., Puxty, G., 2015. Catalysis of CO2absorption in aqueous solution by vanadate and sulfate and their application to post combustion capture. Int. J. Greenh. Gas Control 36, 60–65.

Pohorecki, R., Moniuk, W., 1988. Kinetics of reaction between carbon dioxide and hydroxyl ions in aqueous electrolyte solutions. Chem. Eng. Sci. 43, 1677–1684.

R. Sabouni, H. Kazemian, S. Rohani, Carbon dioxide capturing technologies: a review focusing on metal organic framework materials (MOFs). Environ. Sci. Pollut. Res. 21(8), 5427–5449 (2014). https://doi.org/10.1007/s11356-013-2406-2

Reay, D. A., Ramshaw, C., & Harvey, A. (2013). *Process intensification: engineering for efficiency, sustainability and flexibility*. Oxford: Butterworth-Heinemann.

Rezazadeh, F., Gale, W.F., Rochelle, G.T., Sachde, D., 2017. Effectiveness of absorber intercooling for CO2absorption from natural gas fired flue gases using monoethanolamine solvent. Int. J. Greenh. Gas Control 58, 246–255.

Ruthiya KC, van der Schaaf J, Kuster BFM, Schouten JC (2003) Mechanisms of Physical and reaction enhancement of mass transfer in a gas inducing stirred slurry reactor. Chem Eng J 96(1–3):55–69.

S. Dragan, Calculation of the effective mass transfer area in turbulent contact absorber. Studia UBB Chemia LXI, 3, Tom I, 2016, pp. 227–238.

Saeed, I.M., Alaba, P., Mazari, S.A., Basirun, W.J., Lee, V.S., Sabzoi, N., 2018. Opportunities and challenges in the development of monoethanolamine and its blends for post-combustion CO2 capture. Int. J. Greenh. Gas Control 79, 212–233.

Scripps Institution of Oceanography, in The Keeling Curve (2017)

Seader JD, Henley EJ, Roper DK. Separation process principles. third ed. John Wiley & Sons; 2010.

Sharma T, Kumar A (2021) Efficient reduction of CO2 using a novel carbonic anhydrase producing Corynebacterium flavescens. Environ Eng Res 26(3):200191.

Sharma T, Sharma S, Kamyab H, Kumar A (2020a) Energizing the CO2 utilization by chemoenzymatic approaches and potentiality of carbonic anhydrases: a review. J Clean Prod 247:119138.

Shen, S., Feng, X., Zhao, R., Ghosh, U.K., Chen, A., 2013. Kinetic study of carbon dioxide absorption with aqueous potassium carbonate promoted by arginine. Chem. Eng. J. 222, 478–487.

Skoczylas, A., Majewski, W., 1991. Effective interfacial area in mechanical thin-layer apparatus. Chem. Eng. J. 46, 69–78.

Song Y, Cao L, Yu J, Zhang S, Chen S, Jiang Y (2017) Amino-functionalized graphene oxide blend with monoethanolamine for efficient carbon dioxide capture. J Alloys Compd 704(2017):245–53.

Spigarelli, B.P., 2013. A NOVEL APPROACH TO CARBON DIOXIDE CAPTURE AND STORAGE.

Sujatha, K., Jain. D. , Kamath, S., Kuipers, J., Deen, N., 2017. Experimental and numerical investigation of a micro-structured bubble column with chemisorption. Chem. Eng. Sci., Chemical Engineering Science 169, 225-234

T.R. Anderson, E. Hawkins, P.D. Jones, CO2, the greenhouse effect and global warming: from the pioneering work of Arrhenius and Callendar to today's Earth System Models. Endeavour 40(3), 178–187 (2016). https://doi.org/10.1016/j.endeavour.2016.07.002

Tan LS, Shariff AM, Lau KK, Bustam MA (2012) Journal of industrial and engineering chemistry factors affecting CO2 absorption efficiency in packed column: a review. J Ind Eng Chem 18(6):1874–1883.

Tavan, Y., Hossein, S., 2017. A novel rate of the reaction between NaOH with CO 2 at low temperature in spray dryer. Petroleum 3, 51–55.

Thaker, K., Rao, D.P., 2007. Effects of gas redispersion and liquid height on gas-liquid hydrodynamics in a multistage bubble column. Chem. Eng. Res. Des. 85, 1362–1374.

Thakur, R.K., Vial, C., Nigam, K.D.P., Nauman, E.B., Djelveh, G., 2003. Static mixers in the process industries - a review. Chem. Eng. Res. Des. 81, 787–826.

Thee, H., Smith, K.H., Silva, G. da, Kentish, S.E., Stevens, G.W., 2015. Carbonic anhydrase promoted absorption of CO 2 into potassium carbonate solutions. Greenh. Gases Sci. Technol. 2, 108*114.

Thee, H., Suryaputradinata, Y.A., Mumford, K.A., Smith, K.H., Silva, G. da, Kentish, S.E., Stevens, G.W., 2012. A kinetic and process modeling study of CO2capture with MEA-promoted potassium carbonate solutions. Chem. Eng. J. 210, 271–279.

Tokumura, M., Baba, M., Kawase, Y., 2007. Dynamic modeling and simulation of absorption of carbon dioxide into seawater 62, 7305–7311.

Tsai, C.Y., Chen, Y.S., 2015. Effective interfacial area and liquid-side mass transfer coefficients in a rotating bed equipped with baffles. Sep. Purif. Technol. 144, 139–145.

Vaidya, P.D., Kenig, E.Y., 2007. CO2-alkanolamine reaction kinetics: A review of recent studies. Chem. Eng. Technol. 30, 1467–1474.

Vàzquez, G., Cancela, M.A., Riverol, C., Alvarez, E., Navaza, J.M., 2000. Determination of interfacial areas in a bubble column by different chemical methods. Ind. Eng. Chem. Res. 39, 2541–2547.

Verma P, Arunachalam K, Kumar A, Davery A (2020) Microbial fuel cell – a sustainable approach for simultaneous wastewater treatment and energy recovery. J Water Process Eng 101768.

Versteeg, G.F., VAN DIJCK, L.A.J., VAN SWAAIJ, W.P.M., 1996. ON THE KINETICS BETWEEN CO 2 AND ALKANOLAMINES BOTH IN AQUEOUS AND NON-AQUEOUS SOLUTIONS. AN OVERVIEW. Chem. Eng. Commun. 144, 113–158

W.H. Tay, K.K. Lau, L.S. Lai, A.M. Shariff, T. Wang, Current development and challenges in the intensified absorption technology for natural gas purification at offshore condition, J. Nat. Gas Sci. Eng. 71 (2019).

Wang M, Lawal A, Stephenson P, Sidders J, Ramshaw C. Post-combustion CO2 capture with chemical absorption: a state-of-the-art review. Chem Eng Res Des 2011;89:1609–24.

Wang T, Wei Y, Fang M, He H, Xiang Q, Ma Q, Xia M, Luo Z, Cen K (2012) Wetted-Wall column study on CO2 absorption kinetics enhancement by additive of nanoparticles. Greenhouse Gases Sci Technol 2(5):352–368.

Weiland, R.H., Ahlgren, K.R., Evans, M., 1993. Mass-Transfer Characteristics of Some Structured Packings. Ind. Eng. Chem. Res. 32, 1411–1418.

Westerterp, K.R., Swaaij, W.P.M., Beenackers, A.A.C.M., 1998. Chemical Reactor Design and Operation. Wiley, New York.

Wong S, Bioletti R. Carbon dioxide separation technologies. Carbon & Energy Management. Alberta Research Council Report; 2002.

Yang, H., Fan, S., Lang, X., Wang, Y., & Nie, J. 2011. Economic Comparison of Three Gas Separation Technologies for CO2 Capture from Power Plant Flue Gas. *Chinese Journal of Chemical Engineering, 19*(4), 615-620. doi:10.1016/s1004-9541(11)60031-1

Yang, H., Xu, Z., Fan, M., Gupta, R., Slimane, R.B., Bland, A.E., Wright, I., 2008. Progress in carbon dioxide separation and capture: A review. J. Environ. Sci. 20, 14–27.

Yang, K., Chu, G., Zou, H., Sun, B., Shao, L., Chen, J.F., 2011. Determination of the effective interfacial area in rotating packed bed. *Chem. Eng. J. 168*, 1377–1382. doi:10.1016/j.cej.2011.01.100

Yoo, M., Han, S., & Wee, J., 2013. Carbon dioxide capture capacity of sodium hydroxide aqueous solution. Journal of Environmental Management, 114, 512-519. doi:10.1016/j.jenvman.2012.10.061

Yoshida, F., Miura, Y., 1963. Effective interfacial area in packed columns for absorption with chemical reaction. AIChE J. 9, 331–337.

Z.E. Zhang, Hollow fiber membrane contactor absorption of CO2 from the flue gas: review and perspective, Global NEST J. 16 (2) (2014) 354–373.

Zendehboudi S, Bahadori A, Lohi A, Elkamel A, Chatzis I. Practical and economic aspects of the ex-situ process: implications for CO2 sequestration. Energy Fuels 2013;27:401–13.

Zendehboudi S, Leonenko Y, Shafiei A, Soltani M, Chatzis I. Modeling of CO2 droplets shrinkage in ex situ dissolution approach with application to geological sequestration: analytical solutions and feasibility study. Chem Eng J 2012;197:448–58.

Zhang Z, Borhani TNG, El-Naas MH. Chapter 4.5 - carbon capture A2 - dincer, ibrahim. In: Colpan CO, Kizilkan O, editors. Exergetic, energetic and environmental dimensions. Academic Press; 2018. p. 997–1016.

Zhao S, Cao C, Wardhaugh L, Feron PHM (2015) Membrane evaporation of amine solution for energy saving in post-combustion carbon capture: performance evaluation. J Membr Sci 473(2015):274–82.

Zhao S, Feron PHM, Deng L, Favre E, Chabanon E, Yan S, Hou J, Chen V, Qi H (2016) Status and progress of membrane contactors in post-combustion carbon capture: a state-of-the-art review of new developments. J Membr Sci 511(2016):180–206.

Zhou S, Wang S, Chen C (2012) Thermal degradation of monoethanolamine in CO2 capture with acidic impurities in flue gas. Ind Eng Chem Res 51(6):2539–2547.

Ziókowski, D., Morawski, J., 1987. The flow characteristic of the liquid streams inside a tubular apparatus equipped with static mixing elements of a new type. Chem. Eng. Process. 21, 131–139.